

## RECOMMENDATION ITU-R BS.1195

## TRANSMITTING ANTENNA CHARACTERISTICS AT VHF AND UHF

(Question ITU-R 76/10)

(1995)

The ITU Radiocommunication Assembly,

*considering*

- a) that, by Resolution 76-1, the ex-CCIR has decided that the results of the studies carried out by Radiocommunication Study Group 10 and the related antenna diagrams should be contained in ITU-R Recommendations separately published;
- b) that comprehensive information on the characteristics of transmitting and receiving antenna systems at VHF and UHF is required for frequency planning;
- c) that computer-based procedures are required to give, in a standardized form, the gain and directivity patterns of transmitting and receiving antenna systems;
- d) that it is essential to verify both the antenna system element radiation pattern and the overall antenna system radiation pattern by measurements;
- e) that standardized measurement methods are required to verify the radiation patterns mentioned in *considering* d);
- f) that differences are to be expected between theoretical and measured performance due to practical aspects of VHF and UHF antennas,

*recommends*

- 1** that the formulae contained in Part 1 of Annex 1 and the associated computer programs described in Part 3 of Annex 1 should be used to evaluate VHF and UHF antenna systems performances for planning purposes;
- 2** that the measurement methods contained in Part 2 of Annex 1 should be used to verify the practical performances of the antenna system elements and of the overall antenna system.

## PART 1

**VHF and UHF transmitting antenna pattern calculation**

## TABLE OF CONTENTS

	<i>Page</i>
<b>1 Introduction</b> .....	3
<b>2 Geometrical representation of antenna radiation patterns</b> .....	3
<b>3 Radiation patterns and gain calculation</b> .....	4
<b>4 Radiating elements</b> .....	5
4.1 Point sources.....	5
4.2 Arrays of point sources.....	6
4.2.1 Pattern multiplication.....	7
4.2.2 Vectorial pattern addition.....	7
4.3 VHF and UHF elementary radiators .....	7
<b>5 Polarization</b> .....	8
5.1 Elliptical polarization.....	9
5.2 Horizontal and vertical polarization .....	9
5.3 Slant polarization.....	9
5.4 Circular polarization .....	10
<b>6 Antenna arrays</b> .....	10
6.1 Broadside arrays .....	10
6.1.1 Linear antenna arrays with parasitic elements .....	14
6.2 The amplitude and phase radiation patterns.....	15
6.3 Calculation of the radiation pattern of antenna arrays.....	17
6.4 VHF and UHF antenna arrays .....	18
6.4.1 Panel type antennas.....	18
6.4.2 Yagi antennas.....	20
6.4.3 Other types of antenna array .....	20
<b>7 Antenna systems</b> .....	20
7.1 The antenna system pattern.....	21
7.1.1 Null filling.....	21
7.1.2 Beam tilting.....	24
7.2 Antenna system radiation patterns.....	24
7.3 Examples of antenna system pattern.....	27
7.3.1 Dipole antenna systems.....	27
7.3.2 Yagi antenna systems.....	28
7.3.3 Panel antenna systems.....	28

PART 1  
TO ANNEX 1

## VHF and UHF transmitting antenna pattern calculation

### 1 Introduction

This Part briefly summarizes the basic theoretical principles of VHF and UHF antennas and the general characteristics of antenna systems realized by a number of individual radiators.

Some examples of antenna systems are also given in order to show their performance and orientate the user in selecting the configuration that best suits the requirements.

In particular § 6.4 and 7.2 give the analytical procedure to calculate the overall radiation pattern of an antenna system. The aim of this section is to provide a recommended unified approach to evaluate the performance of an antenna system in ideal conditions.

However, it is to be borne in mind that deviations from the patterns calculated according to the above procedure can be encountered in practical situations as described in Part 2.

### 2 Geometrical representation of antenna radiation patterns

An antenna can consist of a single element or an array of radiating elements. The spatial radiation distribution, or pattern, of an antenna can be represented by a three-dimensional locus of points, with each point having a value of cymomotive force (c.m.f.)\*, based on a half-sphere above the ground centred at the antenna and of radius which is large compared to the physical and electrical dimensions of the antenna.

The c.m.f. at a point on the sphere is indicated in dB below the maximum c.m.f., which is labelled 0 dB.

The three-dimensional radiation pattern is based on the reference coordinate system of Fig. 1.

In a spherical polar coordinate system the following parameters are defined:

$\theta$ : elevation angle from the horizontal ( $0^\circ \leq \theta \leq 90^\circ$ )

$\varphi$ : azimuthal angle from the x-axis ( $0^\circ \leq \varphi \leq 360^\circ$ )

$r$ : distance between the origin and the observation point

Q: observation point.

---

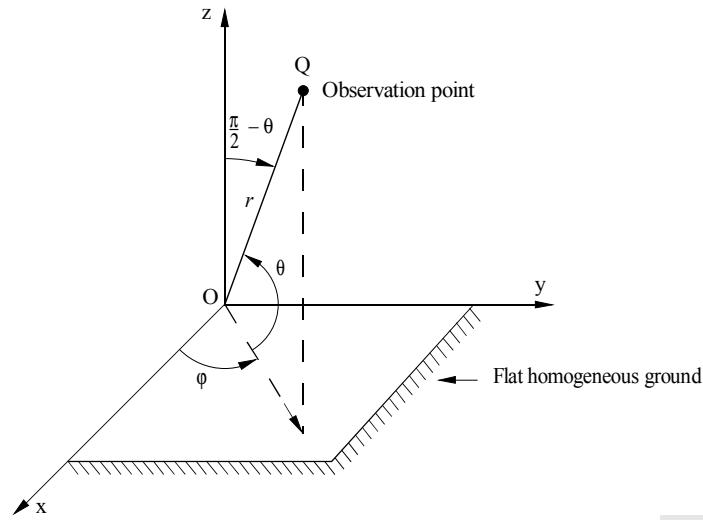
\* Definition of cymomotive force and specific cymomotive force (see Recommendation ITU-R BS.561).

The cymomotive force at a given point in space is the product of the electric field strength at that point produced by the antenna and the distance from that point to the antenna. This distance must be large enough for the reactive components of the field to be negligible.

The c.m.f.(V) is numerically equal to the electric field strength (mV/m) at a distance of 1 km.

The specific cymomotive force at a point in space is the c.m.f. at that point when the power radiated by the antenna is 1 kW.

FIGURE 1  
The reference coordinate system



D01

### 3 Radiation patterns and gain calculation

In the reference coordinate system of Fig. 1, the magnitude of the electrical field contributed by an antenna is given by the following expression:

$$|E(\theta, \varphi)| = k |f(\theta, \varphi)| \quad (1)$$

where:

$|E(\theta, \varphi)|$ : magnitude of the electrical field

$|f(\theta, \varphi)|$ : radiation pattern function

$k$ : normalizing factor to set  $|E(\theta, \varphi)|_{max} = 1$ , i.e. 0 dB

Expressing the total electrical field in terms of its components in a spherical coordinate system, gives:

$$|E(\theta, \varphi)| = \left[ |E_{\theta}(\theta, \varphi)|^2 + |E_{\varphi}(\theta, \varphi)|^2 \right]^{1/2} \quad (2)$$

The directivity,  $D$ , of a radiating source is defined as the ratio of its maximum radiation intensity (or power flux-density) to the radiation intensity of an isotropic source radiating the same total power. It can be expressed by:

$$D = \frac{4\pi |E(\theta, \varphi)_{max}|^2}{\int_0^{2\pi} \int_0^{\pi} |E(\theta, \varphi)|^2 \cos \theta \, d\theta \, d\varphi} \quad (3)$$

When equation (1) is applied,  $D$  can be expressed in terms of the normalized radiation pattern function of the source,  $|f(\theta, \varphi)|$ :

$$D = \frac{4\pi |f(\theta, \varphi)_{max}|^2}{\int_0^{2\pi} \int_0^{\pi} |f(\theta, \varphi)|^2 \cos \theta \, d\theta \, d\varphi} \quad (4)$$

The above definition of directivity is a function only of the shape of the source radiation pattern.

To take into account the antenna efficiency, it is necessary to define its gain  $G$ , expressed as a ratio of its maximum radiation intensity to the maximum radiation intensity of a reference antenna with the same input power.

When a lossless isotropic antenna is taken as the recommended reference antenna, the gain,  $G_i$ , is expressed by:

$$G_i = 10 \log_{10} D \quad \text{dB} \quad (5)$$

Another expression used in practice is the gain relative to a half-wave dipole,  $G_d$ , that is:

$$G_d = G_i - 2.15 \quad \text{dB} \quad (6)$$

## 4 Radiating elements

### 4.1 Point sources

When the radiation from an antenna is in the far field condition (Fraunhofer zone), i.e. when the distance from the antenna is such that its electromagnetic fields can be taken as being orthogonal to the direction of propagation, the antenna can be considered as a point source.

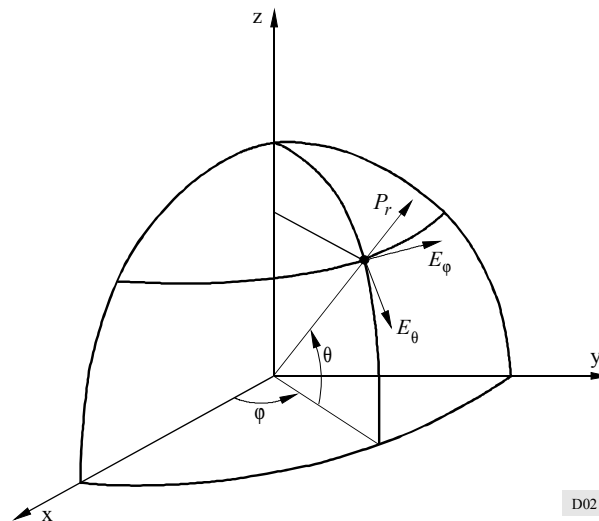
At VHF and UHF, this distance is usually so small that, particularly in the service area, any radiating element can be considered as a point source, regardless of its size and complexity.

Furthermore, the radiation pattern of these point sources, used as an approximation of typical VHF and UHF radiating elements, is usually directional.

In far field conditions the power flux from a point source is always radial.

The Poynting vector results therefore only from two transverse electrical field components  $E_\theta$  and  $E_\phi$  as shown in Fig. 2.

FIGURE 2  
Relation of the Poynting vector and the electrical far field components



D02

When the spherical wave front is at a sufficiently large distance that it can be considered as a plane, the average Poynting vector (radial component only)  $P_r$  is given by:

$$P_r = \frac{E^2}{2 Z_0} \quad (7)$$

where:

$$E^2 = E_\theta^2 + E_\phi^2 \quad (8)$$

and:

$Z_0$ : intrinsic impedance of free space

$E$ : total electrical field intensity.

Considering the variation of the total electrical field strength at a constant radius, the resulting pattern will be a function of  $\theta$  and  $\phi$ . Normalizing the pattern values with respect to its maximum value (assumed in the direction of maximum radiation) the resulting pattern is called a relative amplitude radiation pattern.

The electrical field strength  $E$  generated at a distance  $r$  by an isotropic source radiating a power  $P_{is}$  is given by (see also Recommendation ITU-R P.525):

$$E = \left[ 30 P_{is} / r^2 \right]^{1/2} \quad \text{V/m} \quad (9)$$

where:

$P_{is}$ : isotropic power (W)

$r$ : distance (m)

The above relation is also known as the free-space propagation condition.

Referring the isotropic radiated power  $P_{is}$  to the half-wave dipole radiated power  $P$ , i.e.,  $P_{is} = 1.64 P$ , the expression of the electrical field strength becomes:

$$E = 7.014 \sqrt{P} / r \quad \text{V/m} \quad (10)$$

Expressing  $E$  in mV/m and  $r$  in m:

$$E = 7.014 \times 10^3 \sqrt{P} / r \quad \text{V/m} \quad (11)$$

or, expressing  $E$  in dB( $\mu$ V/m)

$$E = 20 \log_{10} \left( \sqrt{P} / r \right) + 136.9 \quad \text{dB}(\mu\text{V/m}) \quad (12)$$

Considering a non-isotropic point source, the electrical field strength  $E_{ni}$  radiated in the different directions will be affected by the radiation pattern, so that

$$E_{ni} = f(\theta, \phi) \cdot E_{is} \quad (13)$$

where:

$E_{ni}$ : electrical field strength generated at the observation point Q ( $r, \theta, \phi$ ) by a non-isotropic point source radiating power  $P$

$f(\theta, \phi)$ : relative amplitude radiation pattern function of the non-isotropic point source

$E_{is}$ : electrical field strength generated at the observation point Q by an isotropic point source radiating the same power  $P$

## 4.2 Arrays of point sources

When considering arrays of point sources such as those normally encountered at VHF and UHF where complex antenna systems are often required, the following two cases are of immediate interest:

- a) arrays of non-isotropic, similar point sources;
- b) arrays of non-isotropic and dissimilar point sources.

Case a) refers to arrays whose elements have equal relative amplitude radiation patterns (same shape) oriented in the same direction. This is normally the case of an array of vertically stacked panel antennas (see § 6.4.1) beaming toward the same direction.

Case b) is the most general case where no correlation exists between the relative amplitude radiation patterns of the array sources which may arbitrarily be oriented.

#### 4.2.1 Pattern multiplication

For arrays of non-isotropic but similar point sources (case a) of § 4.2), the principle of pattern multiplication applies. According to this principle, the relative amplitudes of the radiation pattern of an array of non-isotropic but similar point sources is the product of the amplitude pattern of the individual source and that of an array of isotropic point sources, while the total phase pattern results from the sum of the phase patterns of the individual source and that of the array of isotropic point sources.

This can be expressed by:

$$E(\theta, \varphi) = f(\theta, \varphi) \cdot F(\theta, \varphi) \quad \angle \left( f_p(\theta, \varphi) + F_p(\theta, \varphi) \right) \quad (14)$$

where, according to the coordinate system shown in Fig. 1:

$E$ : vector of the electrical field strength

$f(\theta, \varphi)$ : relative amplitude radiation pattern function of the individual source

$f_p(\theta, \varphi)$ : phase radiation pattern function of the individual source

$F(\theta, \varphi)$ : relative amplitude radiation pattern function of the array of isotropic sources (also called array factor)

$F_p(\theta, \varphi)$ : phase radiation pattern function of the array of isotropic sources.

#### 4.2.2 Vectorial pattern addition

When the more general case of an array of dissimilar non-isotropic point sources is considered (i.e. non-isotropic sources having different radiation pattern and/or different orientation of the maximum radiation direction, case b) of § 4.2), the principle of pattern multiplication can no longer be applied.

This is a typical situation for VHF and UHF antenna systems, where the radiating elements (panels, Yagi, etc.) are considered as point sources with similar or dissimilar radiation patterns oriented in different directions.

In this case, the resulting radiation pattern  $E(\theta, \varphi)$  is calculated by a vectorial addition of the radiation (amplitude and phase) of each individual point source at any specified angle, as follows:

$$E(\theta, \varphi) = \sum_{i=1}^n E_i(\theta, \varphi) \quad (15)$$

where

$E_i(\theta, \varphi)$ : radiated electrical field of the  $i$ -th source

$E(\theta, \varphi)$ : resulting field strength.

### 4.3 VHF and UHF elementary radiators

Although elementary radiators are seldom individually used in VHF and UHF broadcasting, a brief survey will be given of the most common elementary radiators which are used to form the majority of the VHF and UHF antenna systems.

The basic radiators are: the dipole, the loop, the slot and the helix.

The dipole is the most common elementary radiator at VHF and UHF.

In the coordinate system of Fig. 3, the field components  $E_\theta$  and  $E_\varphi$  produced by a dipole of length  $\ell$  with sinusoidal current distribution are:

$$E_\theta = -60 j I_0 \frac{e^{-j r \beta}}{r} \cdot \frac{\cos(\beta \ell \sin \varphi \cos \theta) / 2 - \cos \beta \ell / 2}{1 - \sin^2 \varphi \cos^2 \theta} \cdot \sin \varphi \sin \theta$$

$$E_\varphi = 60 j I_0 \frac{e^{-j r \beta}}{r} \cdot \frac{\cos(\beta \ell \sin \varphi \cos \theta) / 2 - \cos \beta \ell / 2}{1 - \sin^2 \varphi \cos^2 \theta} \cdot \cos \varphi \quad (16)$$

where:

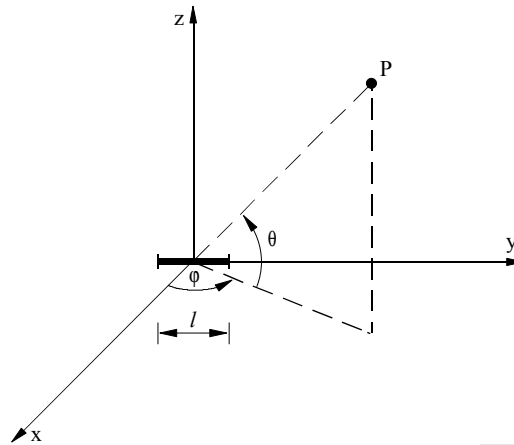
$I_0$ : feed current

$\beta = 2 \pi / \lambda$

$r$ : distance of the point Q of calculation.

The above expression simplifies for  $\ell = 0.5 \lambda$  (see also CCIR Antenna Diagrams, edition 1984).

FIGURE 3  
Elementary dipole in the reference coordinate system



D03

In this case the dipole offers a  $72 \Omega$  resistive impedance at its resonant frequency and can be considered equivalent to a series resonant circuit.

Increasing the diameter of the conductor that forms the arms of the dipole has the effect of increasing the capacity and decreasing the inductance in the equivalent series resonant circuit. Since the Q of the circuit is consequently lowered, the dipole can operate over a wide frequency range.

## 5 Polarization

Traditionally horizontal polarization has been used for FM broadcasting and horizontal or vertical polarization for TV broadcasting.

In recent years, the wide-spread use of FM receivers with built-in antennas and FM car radios has brought about the use of other forms of polarization e.g. circular and slant.

This technique is now also being introduced for TV transmission, especially at UHF, where circular polarization seems to offer better performance in reducing "ghost" images in urban areas.

Report ITU-R BS.464 gives the necessary information for the selection of the most suitable polarization to be used for any new FM service, according to the individual circumstances.

A brief summary of the various forms of polarization is given below to allow for a better evaluation of their differences.

**5.1 Elliptical polarization**

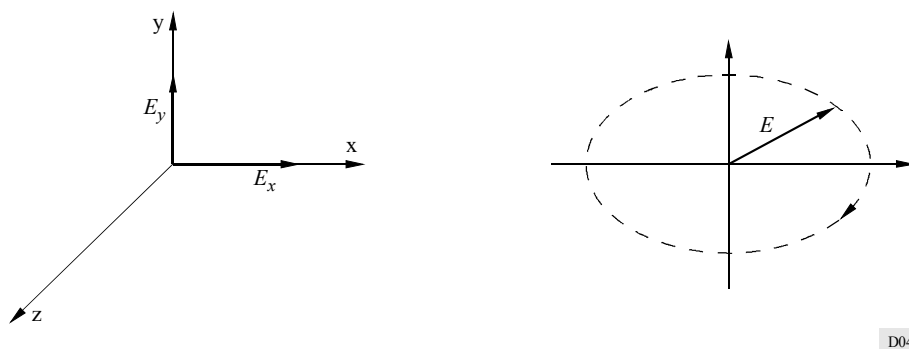
The different forms of wave polarization may be considered as special cases of the more general case of elliptical polarization.

Referring to Fig. 4, an elliptically polarized wave may be represented by two mutually perpendicular linear waves, propagating along the z-axis and having the respective electrical fields expressed by:

$$\begin{aligned}
 E_x &= E_1 \sin \omega t \\
 E_y &= E_2 \sin (\omega t + \varphi)
 \end{aligned}
 \tag{17}$$

where  $\varphi$  is the phase difference between the two waves. When the elliptically polarized wave travels along the z-axis, the resulting  $E$  vector describes an ellipse whose semi-axes are given by  $E_1$  and  $E_2$ .

FIGURE 4  
Elliptical polarization



D04

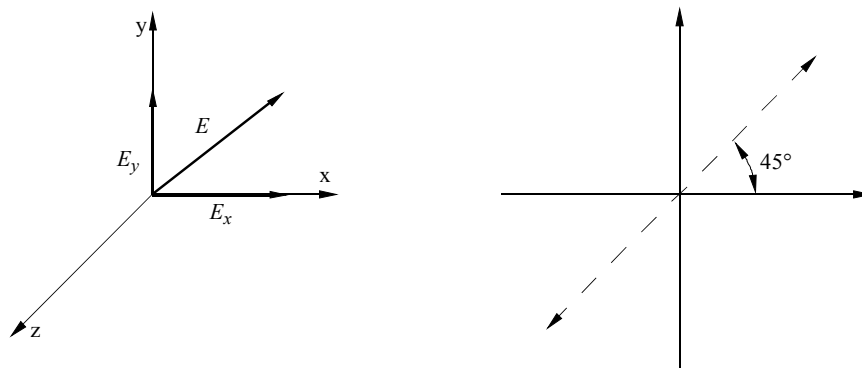
**5.2 Horizontal and vertical polarization**

These two cases occur when in equation (17) either  $E_y = 0$  (horizontal polarization) or  $E_x = 0$  (vertical polarization).

**5.3 Slant polarization**

A 45° slant polarization occurs when in equation (17)  $E_1 = E_2$  and  $\varphi = 0$ .

FIGURE 5  
Slant polarization

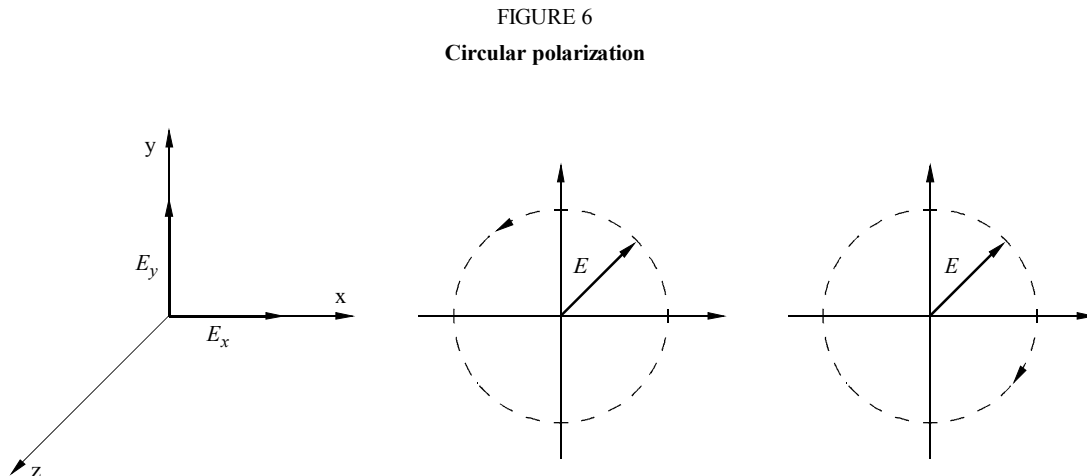


D05

## 5.4 Circular polarization

Circular polarization occurs when in equation (17),  $E_y = E \sin \omega t$  and  $E_x = \pm E \cos \omega t$ . When the sign is positive, the rotation of the wave is clockwise in the positive z-axis direction (right-hand circular polarization).

When the sign is negative, left-hand circular polarization occurs:



D06

Circular or slant polarizations can be produced by using two linearly polarized antennas respectively radiating vertical and horizontal polarization in the appropriate phase relationship as given above.

## 6 Antenna arrays

As mentioned in § 4.3, at VHF and UHF elementary radiators are very seldom used individually and are usually assembled in arrays to achieve:

- higher gain,
- unidirectional pattern.

The most frequently used arrays are linear arrays of elementary radiators. These arrays assembled by the manufacturer, are available to the design engineer in a variety of forms e.g. dipole, Yagi, panel antennas, etc. They are then used to form more complex antenna systems (i.e. arrays of arrays).

In most of the cases these arrays have unidirectional patterns obtained by the use of a reflector which according to the specific case, may be a reflecting metallic surface or a suitable parasitic or active element.

The following sections give some of the fundamental properties of specific linear arrays, which are of immediate use to the designer of antenna systems, e.g. broadside and collinear arrays and linear arrays with parasitic elements.

### 6.1 Broadside arrays

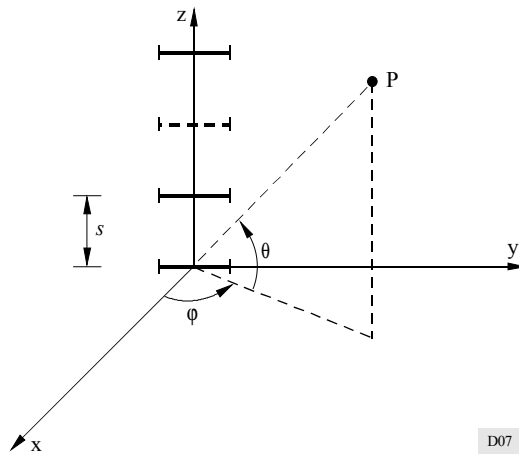
Broadside arrays are easily realized by feeding the elements of a linear array with currents having the same amplitude and phase. The resulting pattern has its maximum (or maxima if no reflector is provided) oriented toward the perpendicular to the line of the array (or to the plane containing the radiating sources).

At VHF and UHF, there are two types of broadside arrays which are of immediate interest to the designer: the horizontal dipole vertical array and the vertical dipole omnidirectional collinear array.

#### *Horizontal dipole vertical arrays*

Horizontal dipole vertical arrays have a repetitive structure (see Fig. 7) consisting of a vertical stack of equally spaced horizontal dipoles (usually  $0.5 \lambda$ ) fed with currents having the same amplitude and phase.

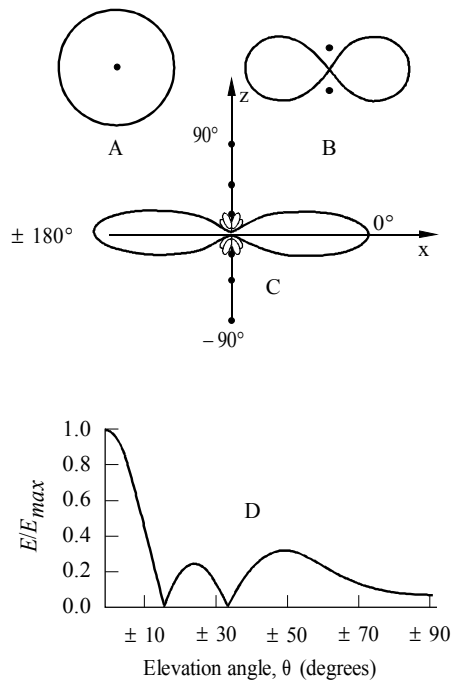
FIGURE 7  
Horizontal dipole vertical array



D07

Typical patterns of this type of array (in the x-z plane) are shown in Fig. 8.

FIGURE 8  
Effect of stacking several point sources having equal currents and phase



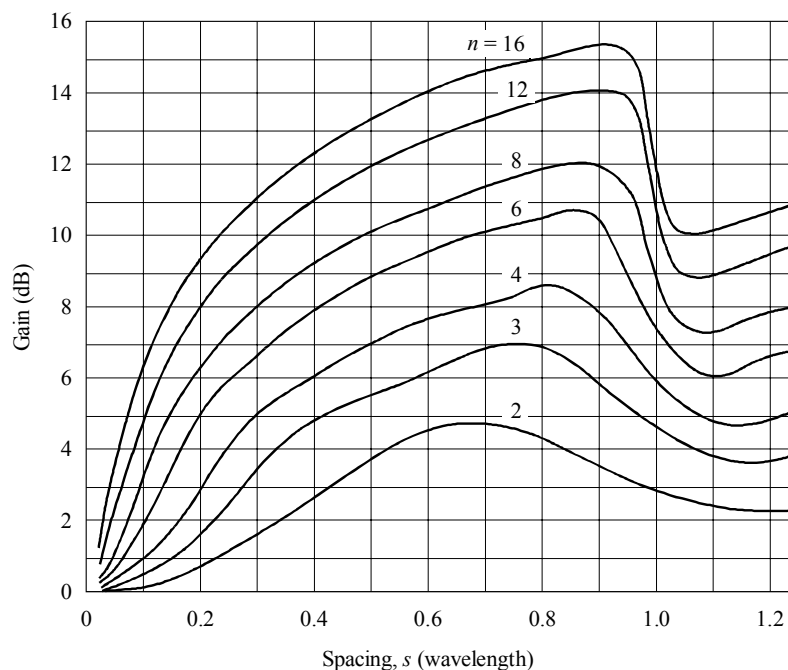
- A: vertical pattern of single source
- B: two sources
- C: six sources
- D: vertical pattern of C in Cartesian coordinates

D08

It is important to note that the gain of the array is a function of the number of elements and their spacing (and hence of the length of the array).

This relationship is shown in Fig. 9, where it can be seen that depending on the value of  $n$ , the optimum spacing lies in the range  $0.65\text{--}0.95\lambda$ . It should be stressed that this optimum spacing is frequency dependent, and that when an antenna system is designed for wide-band (or for adjacent channels) operation, a safety margin should be taken to avoid the steep reduction of gain which occurs at spacing values exceeding the optimum. Usual spacing values for this type of array for individual panel antennas with  $n$  up to 4 elements, are of the order of  $0.5\lambda$ .

FIGURE 9  
Gains of horizontal dipole vertical array (without reflector) as a function of the number  $n$  of elements and their spacing  $s$ .  
The gain is referred to that of a single element



D09

However, when assembling an array of individual radiators (dipoles), the designer can select values closer to the optimum.

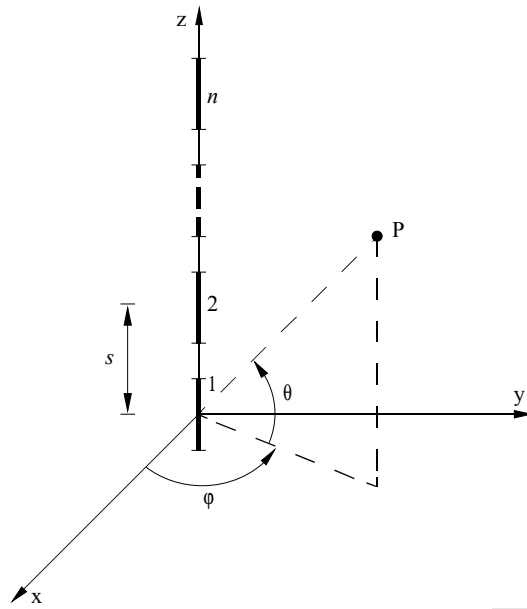
#### *Omnidirectional collinear arrays*

Omnidirectional collinear arrays consist of a vertical stack of equally spaced vertical dipoles fed with currents having the same amplitude and phase (see Fig. 10).

This configuration offers an omnidirectional azimuth pattern and a directive vertical pattern. The overall gain is a function of the number of the elements  $n$  and their spacing  $s$ , as shown in Fig. 11.

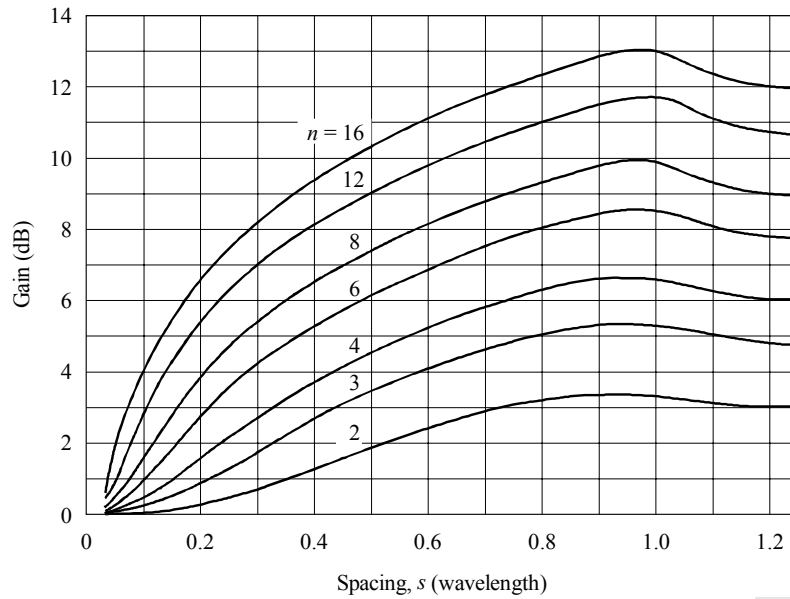
This type of radiating structure is widely used at VHF, especially for omnidirectional antenna systems in FM broadcasting (see also § 7.3.1). It is usually designed by assembling the individual sources (very often folded dipoles), and care should be taken to select the optimum spacing. An adequate margin should be allowed in the case of multichannel operation.

FIGURE 10  
Omnidirectional collinear array



D10

FIGURE 11  
Gain of a vertical collinear array as a function of the number  $n$  of elements and their spacing  $s$ . The gain is referred to that of a single element



D11

### 6.1.1 Linear antenna arrays with parasitic elements

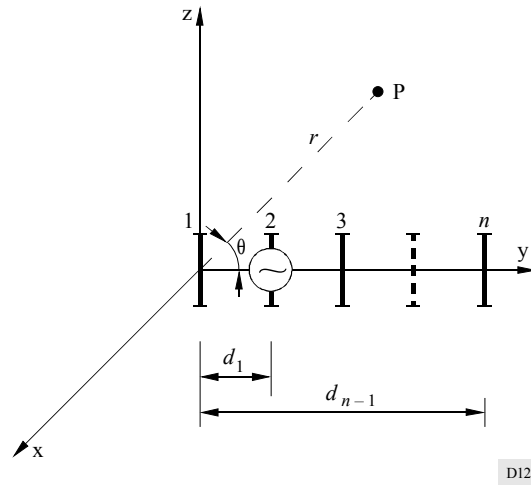
In linear antenna arrays with parasitic elements, the electromagnetic field radiated by the driven element induces currents that flow in the parasitic elements.

At VHF and UHF the most important application of an array with parasitic elements is that represented by the Yagi antenna, schematically shown in Fig. 12.

The Yagi antenna consists of a driven element, a reflector and one or more directors. The overall gain increases with the number of directors that are used.

FIGURE 12

Yagi antenna



NOTE 1 – A quantitative calculation of the pattern can be performed by considering that the  $i$ -th element pattern function of the vertically polarized Yagi antenna shown in Fig. 12 in the  $z$ - $y$  vertical plane is:

$$f_i = \frac{\cos(\beta h_i \cos \theta) - \cos(\beta h_i)}{\sin \theta} \quad (18)$$

where:

$\theta$ : elevation angle

$h_i$ : half-length of the  $i$ -element

$\beta = 2\pi/\lambda$

Since the patterns for each element of a Yagi antenna are different, the principle of pattern multiplication (see § 4.2.1) cannot be used, and it is necessary to carry out a vectorial addition (see also § 4.2.2).

The pattern will be given by:

$$E(\theta, \varphi) = \sum_{i=1}^n I_i \cdot f_i(\theta) \cdot e^{j\beta d_{i-1} \cos \theta} \quad (19)$$

where:

$n$ : total number of dipoles

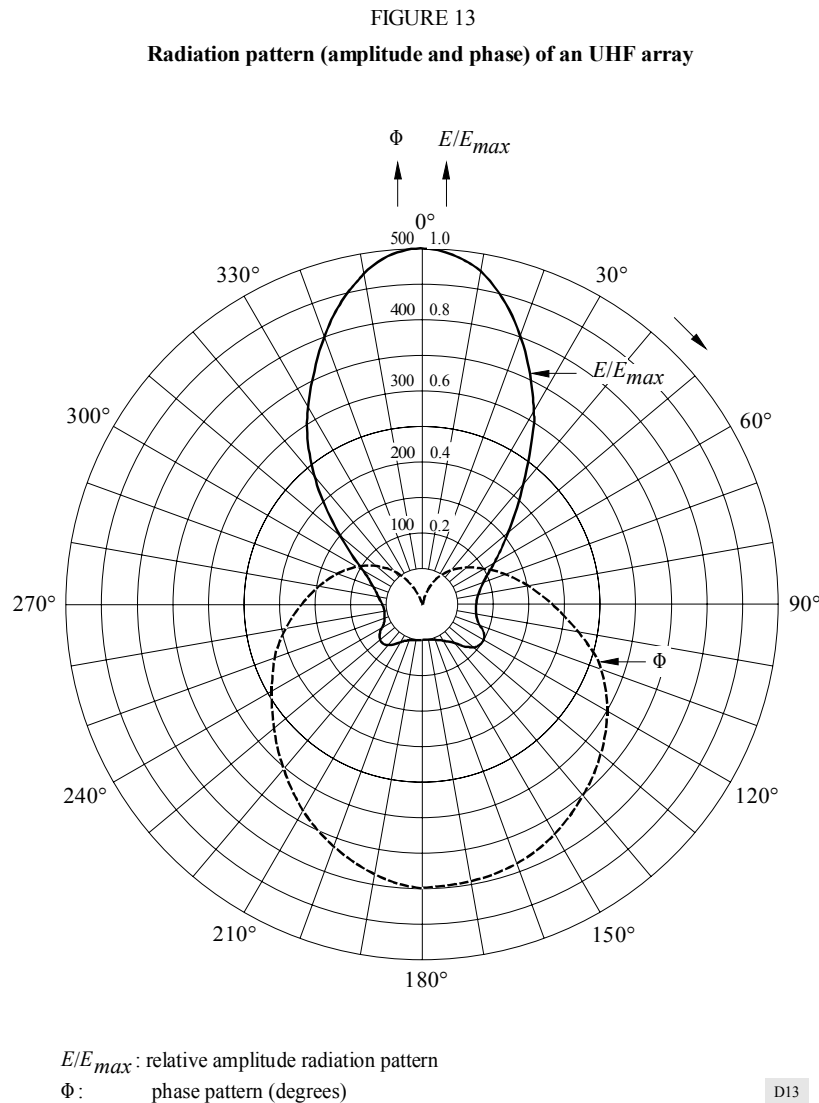
$I_i$ : current in the  $i$ -element

$d_{i-1}$ : distance of the  $i$ -element from the reflector ( $d_0 = 0$ ).

## 6.2 The amplitude and phase radiation patterns

When a single point source is considered, the spatial distribution of the received signal is completely identified by the relative amplitude radiation pattern, i.e. no additional useful information is provided by the associated phase pattern.

In the case of non-isotropic sources of finite size used in an array, the resulting radiation pattern has to be determined by using both the relative amplitude radiation pattern and the associated phase pattern (see Fig. 13).



As mentioned, both the amplitude and phase radiation pattern in the direction of maximum radiation are needed to evaluate the overall antenna pattern. These patterns are normally provided by the manufacturer or measured by the user according to the procedures indicated in Part 2 and should both be used as indicated in § 7.2, to calculate the antenna system pattern.

However, in some cases where an existing system using individual antennas without sufficient technical specifications is to be redesigned or in general when only the relative amplitude pattern is known, the following less accurate approach may be followed.

In this case, the reference point of the radiation i.e., the origin of the relative amplitude radiation pattern, may be suitably transposed to a point called the “phase centre” or the “electrical centre” where the phase pattern shows the least variation over the widest angular sector, i.e., to the actual geometrical centre of the radiated wavefront.

Within this angular sector, the array can be considered as a non-isotropic point source, located at the phase centre, whose radiation pattern can be again completely determined by using only the amplitude radiation pattern.

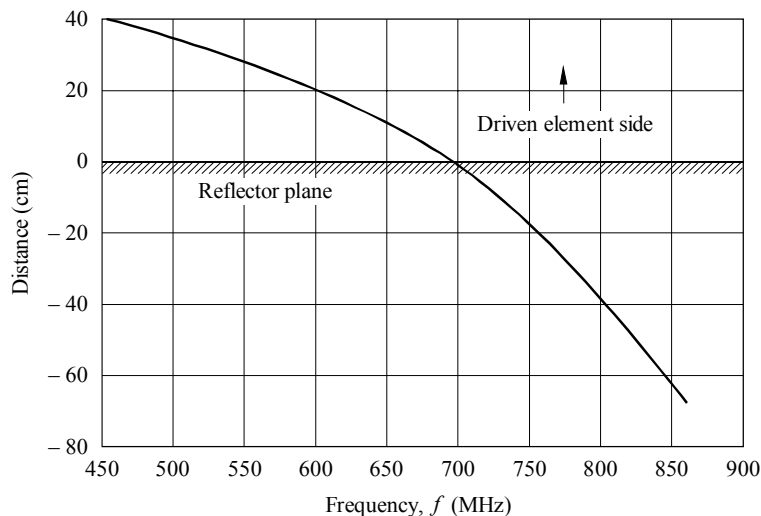
In arrays using dipoles and reflectors, the phase centre usually lies in the zone between the dipole input terminals and the reflecting screen, and typically lies near the dipole terminals.

In the case of a panel array (see § 6.4.1) the exact location of the phase centre, based on measurements, is generally specified by the manufacturer.

Since at VHF and UHF the majority of the individual antennas can operate over relatively large bandwidths (see § 6.4.1), the manufacturer performs the measurements and locates the phase centre for different frequencies in the operating band. From these measurements, a curve is derived which shows the variation of the geometrical position of the phase centre versus frequency (see Fig. 14).

From Fig. 14 it can also be seen the limitations of the phase centre approach when calculating the radiation pattern at directions where large variations in the geometrical position of the phase centre are predicted. This inaccuracy is particularly important at those points where the effects of the combined radiation of more antennas is to be calculated and may considerably alter the resulting radiation pattern where minima and sidelobes are considered.

FIGURE 14  
Location of the phase centre of a wide-band UHF panel antenna

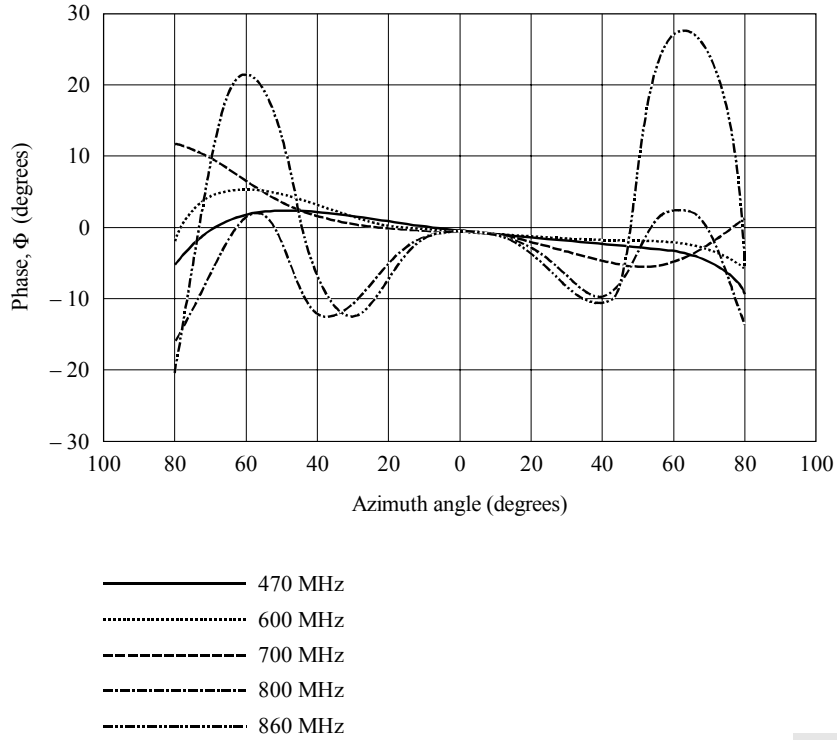


D14

The manufacturer often provides also a family of curves giving the phase patterns obtained at various frequencies. These curves are useful for evaluating the validity of the assumption that a phase centre can be used as the location of the point source in the band concerned (see Fig. 15).

NOTE 1 – In those situations where the phase centre location is not known e.g. old antenna system being re-designed to operate on frequencies different from that of the original design, insufficiently specified radiators, etc., a rule of thumb, often used in the design of antenna systems, consists in placing the phase centre at the feeding terminals of the radiating dipoles. This assumption gives a more conservative result for the overall pattern. It can also be applied to other type of radiating elements e.g. Yagi antennas.

FIGURE 15  
Phase patterns of a wide-band UHF panel antenna  
at various operating frequencies



D15

### 6.3 Calculation of the radiation pattern of antenna arrays

When designing antenna systems with radiators supplied by a manufacturer (simple dipoles, panel or Yagi antennas, etc.), the radiation patterns provided by the manufacturer are usually the vertical and the horizontal section of the 3-dimensional amplitude and/or phase pattern which contains the direction of maximum radiation. Letting  $f_A(\theta, \varphi)$  be the amplitude pattern function of the radiator, the horizontal and vertical radiation patterns can be respectively expressed by:

$$f_{AH}(\varphi) \Big|_{\theta = \theta_{max}} \quad \text{and} \quad f_{AV}(\theta) \Big|_{\varphi = \varphi_{max}} \quad (20)$$

where  $\theta_{max}$  and  $\varphi_{max}$  are respectively the elevation angle and the azimuth angle at which the maximum radiation occurs.

For practical purposes the angles  $\theta_{max}$  and  $\varphi_{max}$  are normally set to zero in the manufacturer's data sheet. The actual values of the amplitude radiation pattern for angles  $\theta \neq \theta_{max}$  and  $\varphi \neq \varphi_{max}$  can be found by the relationship:

$$f_A(\theta, \varphi) = f_{AH}(\varphi) \Big|_{\theta = \theta_{max}} \cdot f_{AV}(\theta) \Big|_{\varphi = \varphi_{max}} \quad (21)$$

In the same way the phase pattern function  $f_P(\theta, \varphi)$  can be expressed by:

$$f_P(\theta, \varphi) = f_{PH}(\varphi) \Big|_{\theta = \theta_{max}} + f_{PV}(\theta) \Big|_{\varphi = \varphi_{max}} \quad (22)$$

where  $f_{PH}(\varphi) \Big|_{\theta = \theta_{max}}$  and  $f_{PV}(\theta) \Big|_{\varphi = \varphi_{max}}$  are respectively the horizontal and vertical phase pattern function of the radiator.

This expression is based on the assumption verified in practice, that any other vertical or horizontal section of the pattern will have a shape similar to the vertical or horizontal section, containing the direction of maximum radiation.

## 6.4 VHF and UHF antenna arrays

### 6.4.1 Panel type antennas

At VHF and particularly at UHF, the dimensions of the elementary radiators are small enough to allow the design of complete antenna systems using elements furnished as a complete product by the manufacturer.

These elements, called panels, are fabricated by the manufacturer by assembling elementary radiators into more complex arrays. The design engineer can then use these panels as “building bricks” for the construction of the final antenna system.

This technique is widely used for modern VHF and UHF antenna system design since it allows for a better control and optimization of the antenna system pattern and hence of spectrum efficiency and economy in the design of the overall system.

A panel may consist of a single simple half-wave dipole mounted at a pre-determined distance from an integral reflecting plane, or for more complicated arrays of 4 (or more) narrow or broad-band, linearly or circularly polarized elementary radiators.

The manufacturer optimizes the panel as regards to:

- gain,
- radiation pattern,
- return loss,
- impedance,
- operating frequency band.

The parameters used in the optimization are:

- physical structure of elementary radiators,
- mutual spacing of elementary radiators,
- distance of the radiators from the reflector (and in some cases the shape of the reflector),
- feeder system.

A very important design characteristic of modern panel antennas is the capability of broadband operation. The same antenna system can often be required to radiate simultaneously more than one programme. This is typically the case for transmitting stations, which are part of a broadcasting network that has to provide two or three programme services to a given area, usually on channels widely spaced in frequency.

This constraint may not be so stringent for FM sound broadcasting in Band II where the required bandwidth is only about  $\pm 10\%$  of the centre frequency, but it considerably affects the design of panels required to fully cover both Bands IV and V (470-960 MHz).

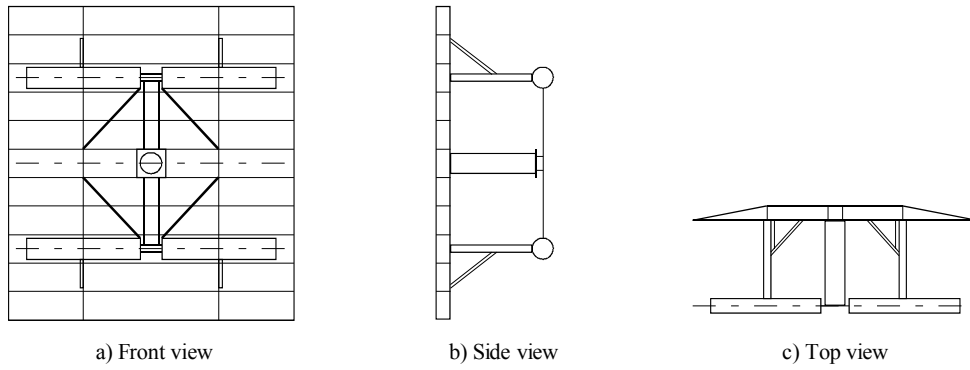
In this case a careful design of the elementary radiator is needed in order to lower the Q of its equivalent circuit. This reduction is usually achieved by using radiating elements with large surface or cross-section area.

A typical design of VHF panels is shown in Fig. 16. It consists of two vertically stacked, centre-fed, full wavelength dipoles. The corresponding vertical and horizontal radiation patterns are shown in Fig. 17.

Typical gain values (referred as usual to the half-wave dipole) for the Band I panels are between 5 to 7 dB, while the Band II panels have an upper limit of the order of 8 dB at the highest operating frequencies. The Band III panels are capable of operation over the full bandwidth of 174-230 MHz and have gain figures of from 10 to 14 dB with a slight reduction in the case of vertical polarization.

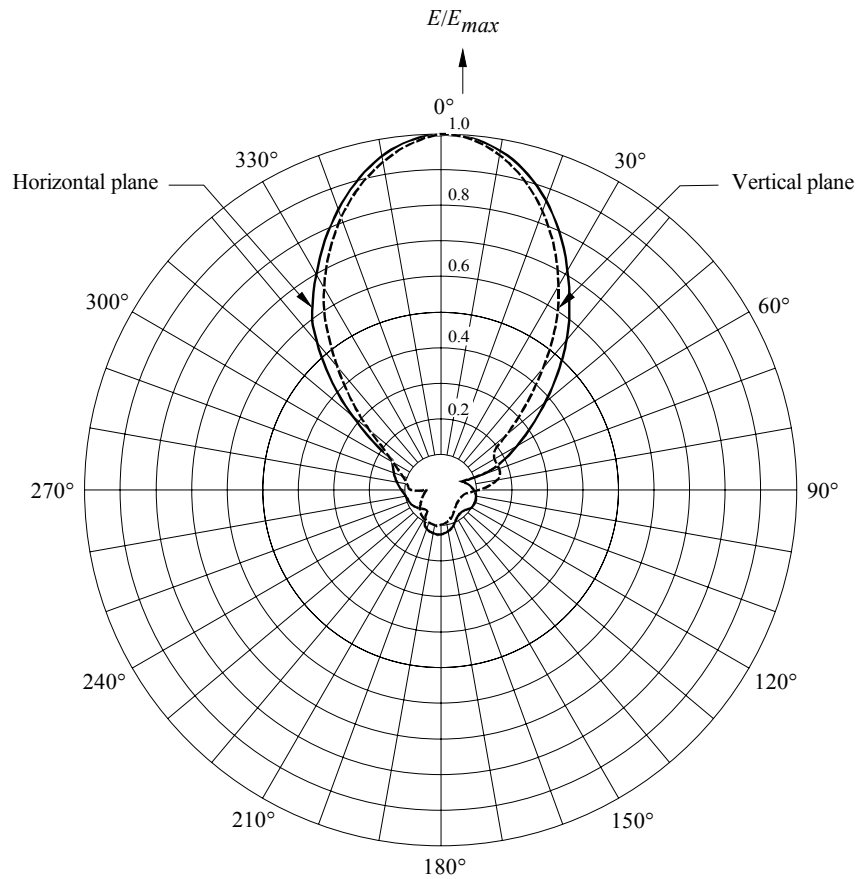
At UHF the reduced size of the radiating elements allows the construction of panels with more directional radiation patterns. At these frequencies, despite the constraints imposed by the requirement for broad-band operation, the technique of stacking centre-fed full-wavelength dipoles is still widely used.

FIGURE 16  
 Typical Band I or Band II dipole panel



D16

FIGURE 17  
 Vertical and horizontal radiation patterns of the dipole panel of Fig. 16



D17

The requirement for broad-band operation has an impact also on the impedance, gain and phase centre location of the panel, and their variation with frequency should be given by the manufacturer. Typical gain values are between 10 to 12 dB, with VSWR values at the panel input not exceeding 1.10.

The demand to broadcast circularly polarized TV emissions has stimulated the development of suitable circularly polarized panels to meet the following requirements:

- the use, when possible, of dipoles as elementary radiators for simplicity of construction;
- provision of similar vertical and horizontal patterns over a wide frequency bandwidth;
- reduction of the mutual coupling between adjacent panels to allow for less complicated designs;
- provision of a pattern shape also suitable for the realization of omnidirectional patterns with minimum ripple.

The preferred approach is still one using a panel comprised of crossed dipoles although this solution has some limitations due to different vertical and horizontal radiation patterns.

#### **6.4.2 Yagi antennas**

Broadcast-type transmitting Yagi antennas usually consist of a driven element (typically a 0.5 wavelength dipole), a reflector to make the pattern unidirectional and one or more directors to increase gain.

Although Yagi antennas cannot strictly be defined as broadband antennas in terms of the considerations expressed in § 6.4.1, they can be designed to operate over a bandwidth around the design frequency that may vary from  $\pm 5$  to  $\pm 10\%$ .

Current designs of Yagi antennas provide full coverage of Band II or coverage of two adjacent TV channels in Band III with a single antenna, with gain values of the order of 4 to 5 dB, depending on the number of directors (1 to 3).

A typical Yagi antenna for FM broadcasting and its associated radiation pattern is shown in Figs. 18a) and 18b).

Another advantage of the Yagi antenna is that it can easily be adapted for use with circular polarization, by arranging cross elements.

Like the panel radiators, Yagi antennas can be used as radiating elements to form more complex antenna systems. They can be arranged in stacks or bays to form arrays whose overall pattern can conform to specific requirements. The resulting pattern can be calculated according to § 4.2, in which the Yagi antennas in the system are considered as non-isotropic point sources located at their respective phase centre, usually assumed to be at the input of the driven element.

#### **6.4.3 Other types of antenna array**

Among the antenna arrays used in VHF broadcasting antenna systems the log-periodic antenna has also found interesting applications in transposer systems both as receiving and as transmitting antenna.

The inherent wide-band operation capabilities of the log-periodic antenna allows for the realization of devices able to easily operate over a full broadcasting band.

The overall performance of typical log-periodic antennas is comparable to that of vertically stacked double Yagi antennas.

## **7 Antenna systems**

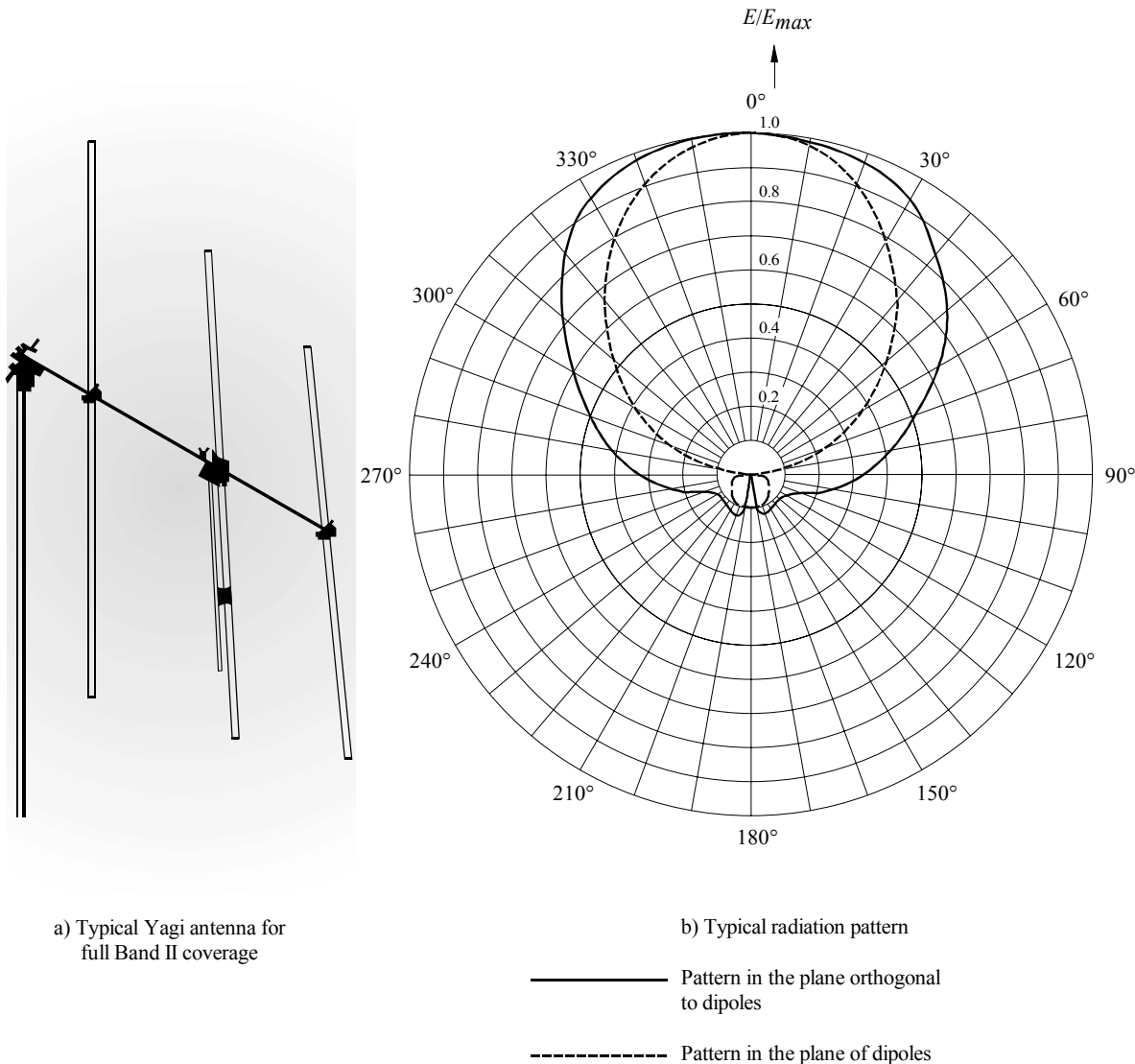
At VHF and UHF, antenna systems are designed by using arrays of radiating elements in order to achieve an optimized radiation pattern.

It is evident that since the signal radiated by the antenna system propagates, to a first approximation, in a line-of-sight mode, all the energy radiated above the horizontal plane containing the antenna, is lost. This loss can be reduced by narrowing the vertical radiation pattern of the antenna system and tilting the beam downward.

In a similar way, the azimuth pattern may also need to be controlled, since it should conform to the required service area and provide the necessary protection to other co-channel or adjacent-channel transmitting stations.

The most efficient solution for controlling both radiation patterns is to arrange for a suitable number of radiating elements e.g. panels, Yagis, etc. to be distributed and/or orientated in the required azimuth direction.

FIGURE 18



D18

The following sections are therefore aimed at providing a survey of the current techniques most often used for the design of optimized antenna systems.

Although specific reference will be made to panel type antenna systems, the considerations given are generally applicable to any technique using radiating elements whose mutual geometrical position and feeding characteristics can be varied by the designer to achieve the wanted overall pattern.

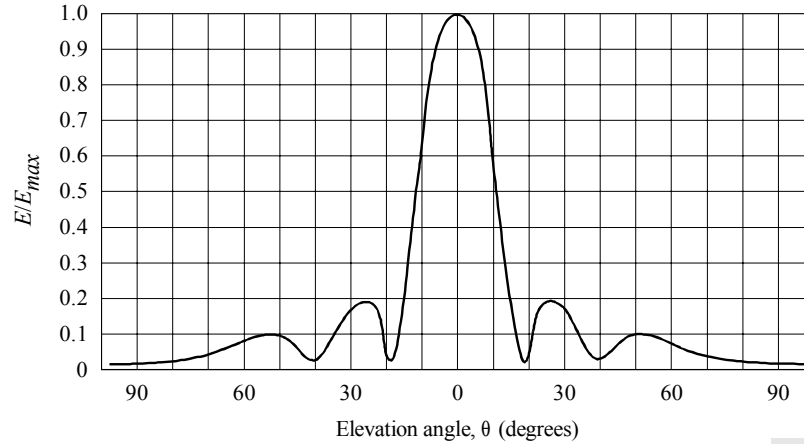
**7.1 The antenna system pattern**

**7.1.1 Null filling**

In the angular sector corresponding to the required service area, the vertical radiation pattern should not contain any nulls, since their presence will result in a theoretically zero signal strength at the locations which coincide with the angles where the nulls occur. In practice, the received signal strength will be considerably less than is required as it will result from uncontrolled reflections from outside the null area.

A typical vertical radiation pattern for a vertical stack of equally spaced radiating elements fed with currents of equal amplitude and phase (i.e. a broadside array, see § 6.1), is shown in Fig. 19. It can be seen that the nulls will affect a considerable portion of the angular sector that could correspond to the required service area.

FIGURE 19  
Vertical radiation pattern for an array of 5 vertical  $0.5\lambda$  spaced radiating elements having equal current and phase



D19

The angles at which nulls occur are given by the approximate formula:

$$\theta = \arcsin \frac{\pm k}{n d} \quad (23)$$

where:

- $k$ : number of the null (1,2, ...)
- $n$ : number of stacked elements
- $d$ : element spacing in wavelengths.

Various “null-filling” techniques have been developed so as to obtain a vertical pattern which approaches the ideal shape described earlier.

The simplest and most widely-used solution consists of feeding the various stacked elements with currents of unequal amplitude, i.e. with a suitable power distribution.

A well-known power distribution technique is the so-called “binomial distribution” which sets the amplitudes of the feed currents proportional to the coefficients of a binomial series.

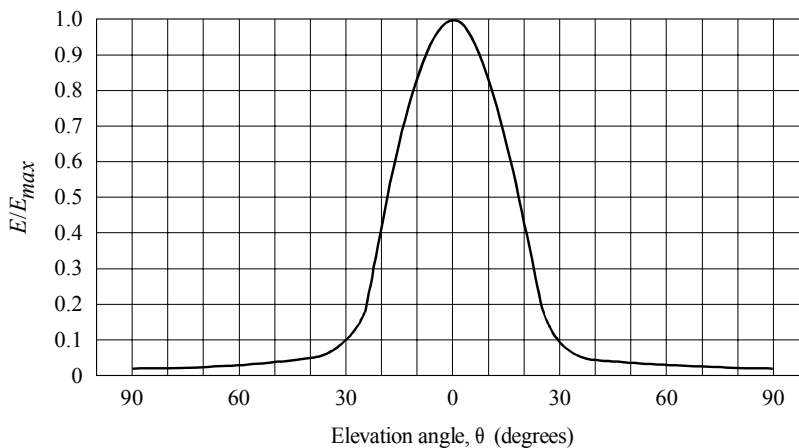
According to the above distribution law, for arrays of 3 to 6 stacked elements, the relative amplitudes of the feed currents are given by:

$n$	Relative amplitude
3	1, 2, 1
4	1, 3, 3, 1
5	1, 4, 6, 4, 1
6	1, 5, 10, 10, 5, 1

Figure 20 shows the vertical pattern of the array of Fig. 19 when a binomial distribution is applied.

Although nulls and minor lobes are eliminated by the binomial distribution, the array beamwidth and consequently its directivity, is decreased. In addition, the changes in the current amplitudes required for large arrays may be quite large. This can create difficulties in realizing and maintaining the stability of the necessary different levels of power.

FIGURE 20  
**Vertical radiation pattern of the array of Fig. 19 when a binomial amplitude distribution is applied**



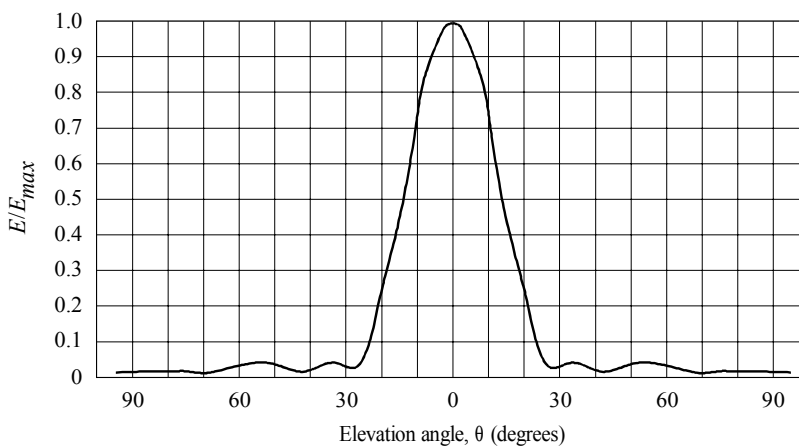
D20

Another power distribution technique that overcomes the above disadvantages is the Dolph-Chebyshev distribution.

When applying this distribution it is necessary either to specify the required maximum sidelobe level if the beamwidth between the first nulls is to be minimized, or conversely, to specify the beamwidth between the first nulls so as to minimize the side lobe levels.

Figure 21 shows the vertical pattern of the array of Fig. 19, when a Dolph-Chebyshev amplitude distribution of 1, 1.6, 1.9, 1.6, 1 corresponding to a specified maximum sidelobe suppression of 27 dB, is applied.

FIGURE 21  
**Vertical radiation pattern of the array of Fig. 19 when a Dolph-Chebyshev amplitude distribution is applied**



D21

The optimum element spacing for this form of distribution is around  $0.5 \lambda$ , although the distribution also holds for larger spacings.

It should be noted that any null-filling technique that is used, will result in a gain reduction with respect to the uniform distribution case.

This gain reduction is usually called “distribution loss”.

This loss can be minimized by suitable pattern synthesis techniques in which the power for null-filling is taken from the portion of the pattern that lies above the horizon or from the compensation of ripples in the main beam.

Other more complicated null-filling techniques combine a suitable phase distribution with the necessary amplitude distribution.

In this more general distribution, the gain loss with respect to the uniform power and equal phase distribution case, is usually called a “compensation loss”.

### 7.1.2 Beam tilting

Beam tilting is necessary not only to reduce the amount of power radiated above the horizontal plane, but also to direct the maximum power toward the Earth’s surface.

In fact, due to the curvature of the Earth, the maximum radiation of an antenna array without any beam tilting would never actually reach the Earth’s surface.

The beam of an antenna located at 300 m above ground level should be tilted at an angle of more than  $0.5^\circ$  to allow the maximum radiation to reach the Earth’s surface.

Small beam tilt angles ( $1^\circ$  to  $3^\circ$ ) are easily implemented by a simple mechanical tilt of the plane of the radiating elements. Larger mechanical tilt angles are not frequently used due to the associated mechanical and environmental difficulties.

Beam tilting can also be achieved by properly controlling the phase of currents feeding the elements in the stack. This control can be realized either by feeding the lower half of the stack elements with currents having a fixed-phase lag with respect to the currents feeding the upper half, or by introducing a progressive phase shift in the current of each adjacent radiating element.

The largest tilt angles are normally achieved by a suitable combination of mechanical and electrical tilting. It should be noted that the introduction of an unequal phase distribution in the radiating elements will result in a “compensation” loss with respect to the gain when a uniform power (and equal phase) distribution is used.

## 7.2 Antenna system radiation patterns

As mentioned in § 6.3 and 6.4, the radiating elements composing an antenna system may be considered as non-isotropic point sources located at their phase centre. In this case, the resulting radiation pattern should be calculated, as indicated in § 4.2, by using a vectorial addition that takes into account the individual radiation patterns.

This vectorial addition can be reduced to the solution of a purely geometrical problem when the amplitude and phase of the feed current of each element are known.

First the case of two isotropic radiating sources arbitrarily located in a 3-dimensional space will be used to find the phase difference between the fields radiated as a function of their mutual position, feed current phases and frequency.

The results will be then extended to the more general case of non-isotropic sources. Referring to Fig. 22, where no specific coordinate system has been given, source 1 will be taken as the reference for deriving the phase difference of source 2, when calculating the resulting field at a point P which corresponds to a specific direction.

In Fig. 22,  $1'$  will be the projection of source 1 on the horizontal plane containing source 2. On this plane, the direction of the geographical North, N, passing through  $1'$  has been shown.

The following parameters are used in Fig. 22.

- $d$ : distance between source 2 and the projection  $1'$  of source 1 on the horizontal plane
- $h$ : vertical distance between source 1 and its projection  $1'$
- $\gamma$ : angle in the horizontal plane between  $d$  and the direction of the geographical North
- $\alpha_H$ : angle on the horizontal plane between the direction of the geographical North and the projection of the direction of calculation on the horizontal plane
- $\alpha_V$ : angle on the vertical plane between the direction of calculation and its projection on the horizontal plane.



Considering an array of  $n$  non-isotropic sources, the resulting field pattern in any direction will be given by the vectorial addition of  $n$  vectors whose amplitude will be given by the individual source amplitude radiation pattern and phase given by (26), taking source 1 as reference. In symbols:

$$E(\theta, \varphi) = \sum_{i=1}^n V_i(\theta, \varphi) = \sum_{i=1}^n K_i \cdot f_i(\theta, \varphi) \cdot e^{j\psi_i(\theta, \varphi)} \quad (27)$$

where:

$V_i$ : individual field vector

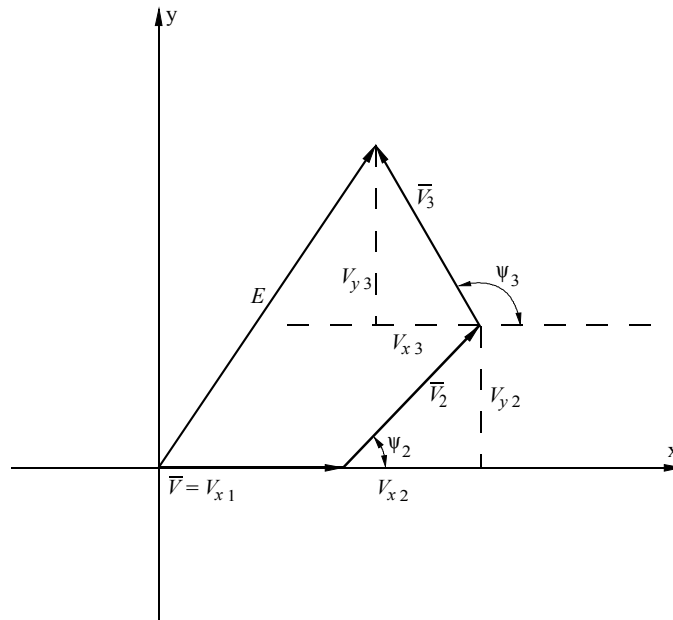
$K_i$ : constant taking into account differences in input powers to the sources

$f_i$ : individual source relative amplitude radiation pattern

$\psi_i(\theta, \varphi)$ : relative phase difference of the  $i$ -source referred to source 1 ( $\psi_1(\theta, \varphi) = \psi_{p1}(\theta, \varphi)$ ).

It may be convenient to perform the vectorial addition in an x-y vectorial plane as shown in Fig. 23, for  $n = 3$ .

FIGURE 23  
x-y plane vectorial addition for  $n = 3$



The resulting vector  $E(\theta, \varphi)$  will have the components:

$$E_x(\theta, \varphi) = \sum_{i=1}^n V_{xi}(\theta, \varphi) = \sum_{i=1}^n k_i \cdot f_i(\theta, \varphi) \cdot \cos \psi_i \quad (28)$$

$$E_y(\theta, \varphi) = \sum_{i=1}^n V_{yi}(\theta, \varphi) = \sum_{i=1}^n k_i \cdot f_i(\theta, \varphi) \cdot \sin \psi_i \quad (29)$$

Hence:

$$|E(\theta, \varphi)| = \left[ |E_x(\theta, \varphi)|^2 + |E_y(\theta, \varphi)|^2 \right]^{1/2} \tag{30}$$

and:

$$\psi(\theta, \varphi) = \arctan \left[ E_y(\theta, \varphi) / E_x(\theta, \varphi) \right] \tag{31}$$

In practice,  $f_i(\theta, \varphi)$  will be calculated according to § 6.3, on the basis of the data supplied by the manufacturer while  $k_i$  will be determined by the power fed to the system and  $\psi_i$  will be calculated according to the geometry of the antenna system and the phase pattern.

Since no specific coordinate system has been initially selected, it is common practice when calculating the phase difference  $\psi_i$ , to refer all the horizontal angles to the North direction and all the vertical angles to the horizontal plane.

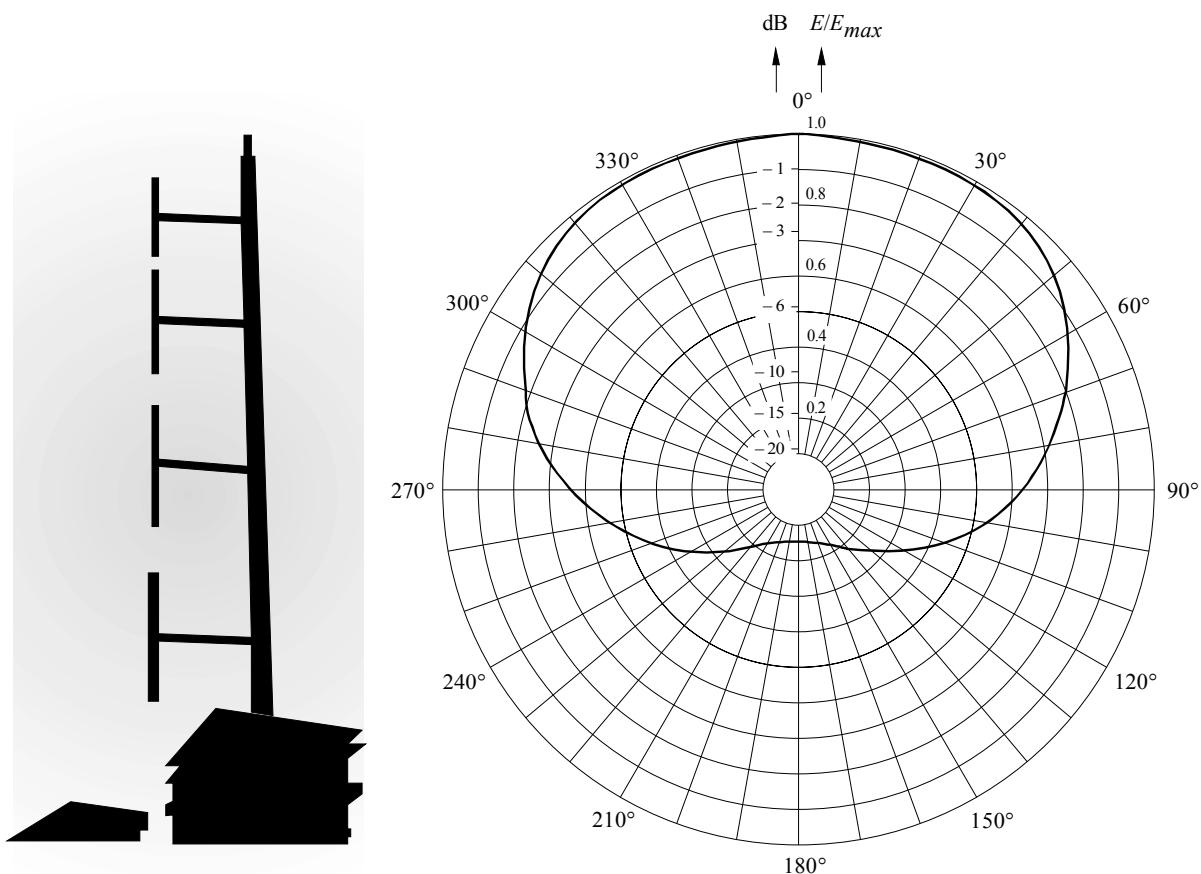
### 7.3 Examples of antenna system pattern

#### 7.3.1 Dipole antenna systems

Dipole antenna systems are widely used in Band II broadcasting. They usually consist in collinear arrays realized by a stack of equally spaced vertical dipoles fed with currents having the same amplitude and phase.

An example of a vertically polarized dipole antenna system and its associated horizontal radiation pattern are shown in Fig. 24.

FIGURE 24  
Vertically polarized Band II dipole antenna



### 7.3.2 Yagi antenna systems

Like panel antennas, Yagi antennas can be used as radiating elements to form more complex antenna systems. They can be arranged in stacks or bays to form arrays whose overall pattern can conform to specific requirements. The resulting pattern can be calculated according to § 4.2, in which the Yagi antennas in the system are considered as non isotropic point sources located at their respective phase centre usually assumed to be at the input of the driven element.

From Fig. 18, it can be easily seen that for the case of horizontally polarized emissions, very poor directivity is obtained in the vertical plane. It is, therefore, common practice to stack Yagi antennas.

Antenna systems having unidirectional or omnidirectional radiation patterns can easily be realised combining Yagi antennas.

An omnidirectional azimuth radiation pattern realised by a 4 Yagi antennas system in Band II is shown in Fig. 25. In this case a suitable technique has also been used to compensate for the minima of the horizontal pattern. This technique consists in adding to the radiating structure 4 passive vertical elements suitably placed in the cross-over directions (see Fig. 26).

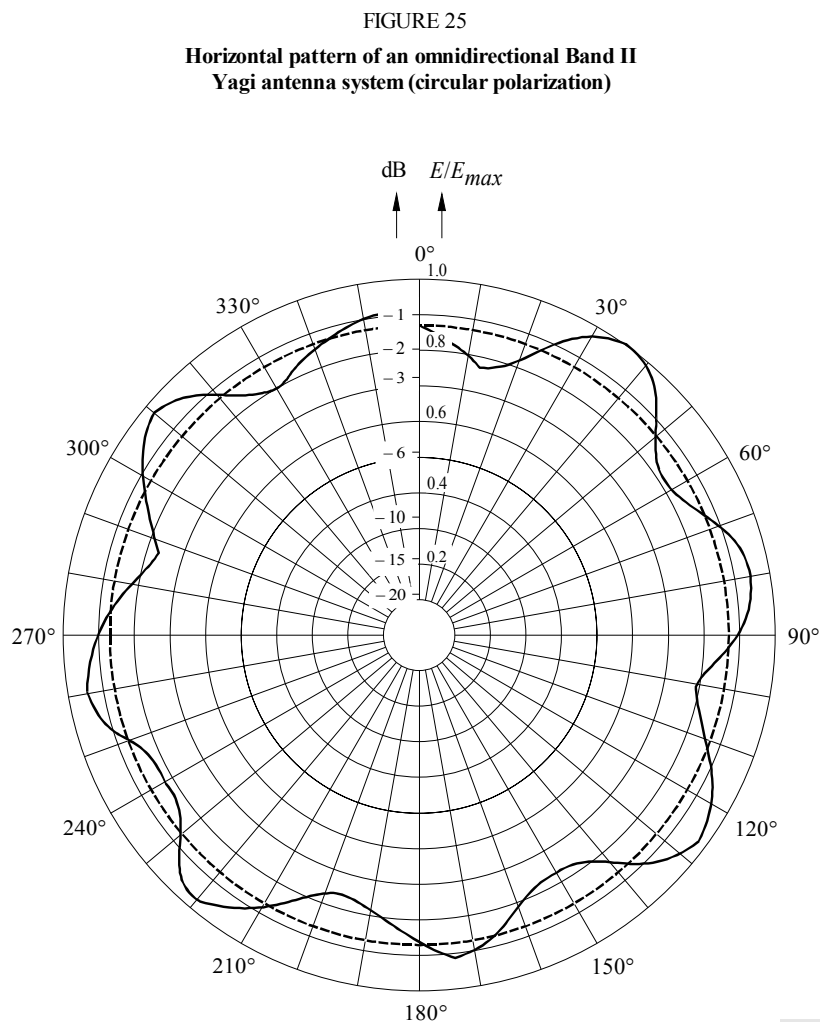
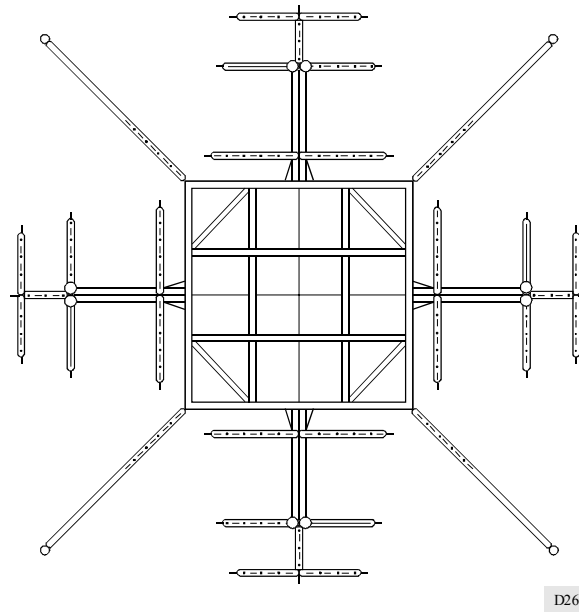


Figure 27 shows a directional azimuth pattern of a 2 Yagi antennas system in Band II.

### 7.3.3 Panel antenna systems

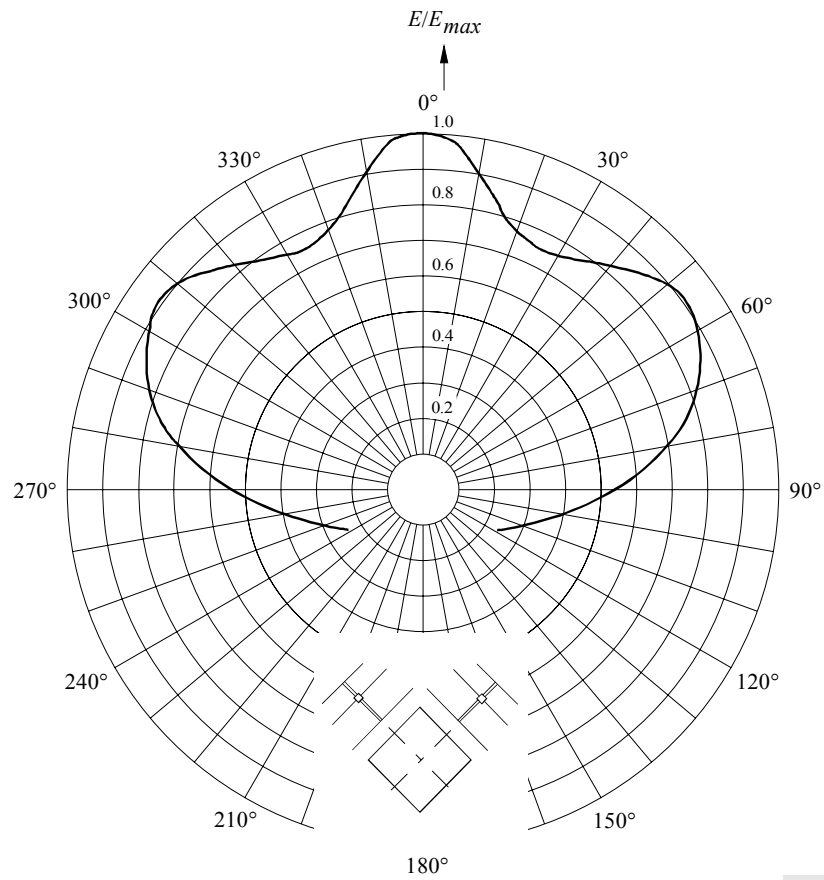
Properly designed panels have unidirectional patterns with the main beam orthogonal to the reflector's surface. The 6 dB beamwidth for panels mounted on towers with square or triangular sections should respectively be 90° or 120°, when an omnidirectional pattern is desired.

FIGURE 26  
**Omnidirectional Yagi antenna system providing  
 the horizontal pattern given in Fig. 25**



D26

FIGURE 27  
**Horizontal pattern of a directional Band II Yagi antenna system**



D27

Thus, when the panels are fed with currents of equal phase in the crossover directions, the combined radiation of two adjacent side-mounted panels compensates for the gain reduction of the individual panel.

### 7.3.3.1 Omnidirectional panel antenna systems

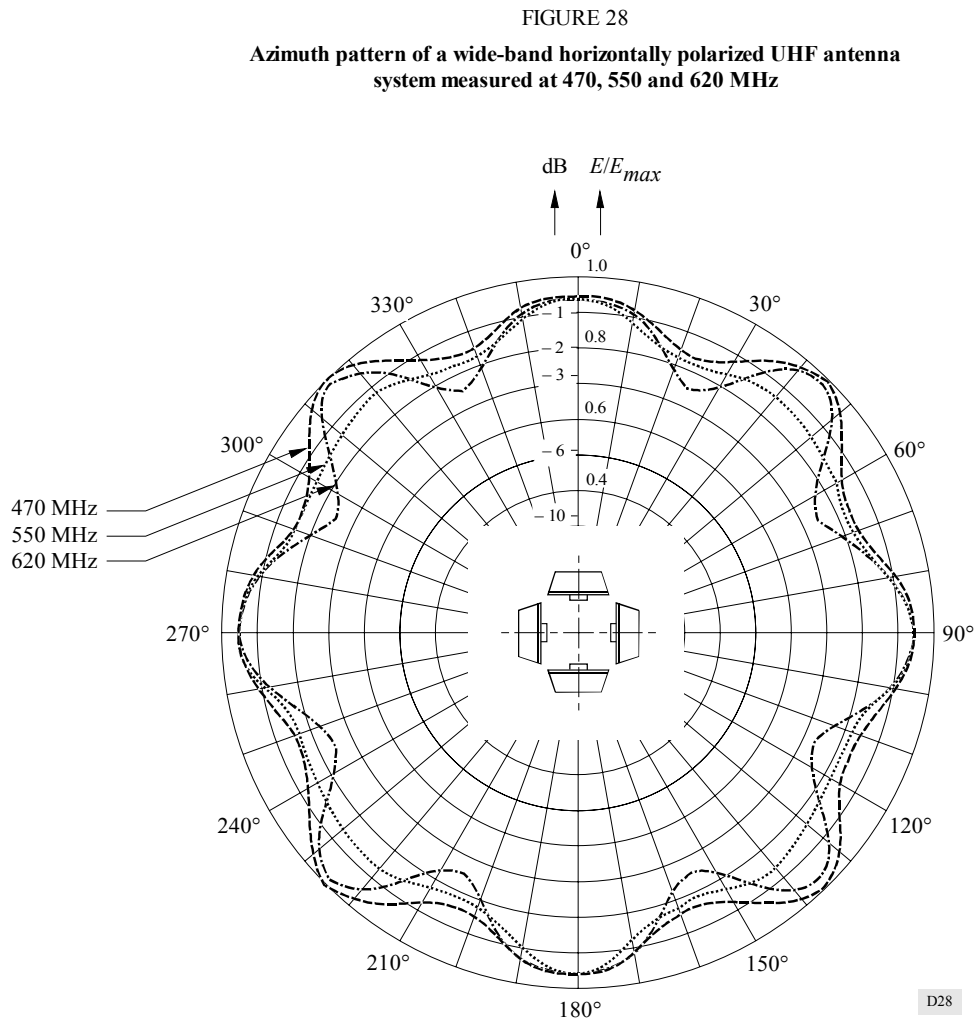
Omnidirectional antenna system patterns can therefore be obtained by feeding the panels of each horizontal section of the array with equal power, the panels being mounted in the centre of the tower sides.

However, the resulting azimuth pattern (see Fig. 28) will have a “ripple” whose amplitude is proportional to the tower side length, expressed in wavelength.

Two main conditions have to be fulfilled when a panel antenna system with an omnidirectional azimuth pattern is designed:

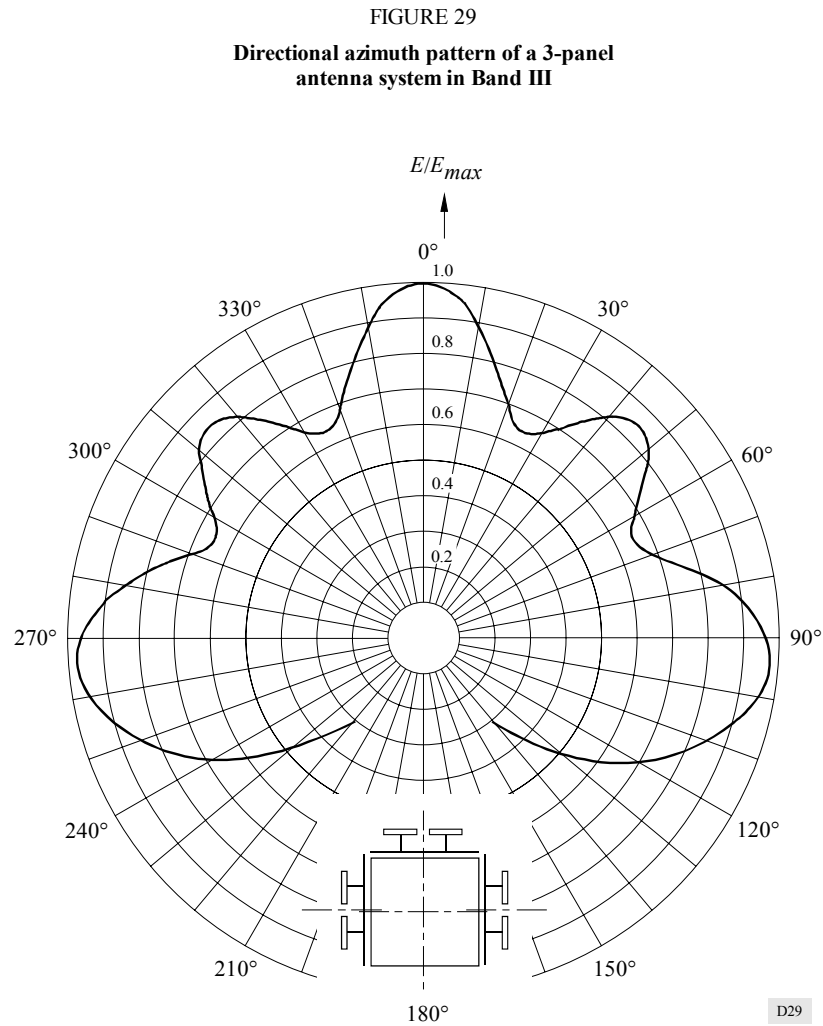
- the irregularities of the azimuth pattern resulting from the radiation of the four panels (or three according to the tower section), should be kept within a specified limit (e.g.  $\pm 1.5$  dB);
- the VSWR at each panel input should be minimized since any mismatch at the branch feeder connections will result in an unequal share of the power among the various panels and the resulting pattern will no longer be circular.

From Fig. 28 it can be seen that the minima of the pattern occur on each side of the crossover directions, where the radiations from adjacent panels have a relative phase shift from each other and the resulting vector has a lower amplitude.



### 7.3.3.2 Directional panel antenna systems

Directional azimuth patterns are obtained by varying the number of panels on each side of the tower, the amount of the power fed to each panel, the mutual orientation of the panels or by a combination of these methods. Figure 29 shows a directional azimuth pattern realized with a 3-panel antenna system at VHF.



PART 2  
TO ANNEX 1

**Practical aspects of VHF and UHF antennas**

TABLE OF CONTENTS

		<i>Page</i>
<b>1</b>	<b>Introduction</b> .....	33
<b>2</b>	<b>Measurement of the characteristics of antenna systems</b> .....	33
2.1	Considerations on the measurement site .....	33
2.2	Parameters to be measured .....	33
2.3	Methods of measurement .....	33
2.3.1	The frequency domain measurement (FDM) method .....	33
2.3.2	Time domain measurement (TDM) method .....	34
2.4	Measuring equipment .....	37
2.5	Measuring procedures .....	37
2.6	Data presentation .....	37
<b>3</b>	<b>On-site measurements of the antenna system characteristics</b> .....	38
3.1	Methods of measurement .....	38
3.1.1	Vertical sounding method .....	40
3.1.2	Airborne method .....	41
3.1.3	Reference antenna method .....	43
3.2	Measuring equipment .....	44
3.2.1	Vertical sounding measuring equipment .....	44
3.2.2	Airborne measuring equipment .....	44
3.2.3	Reference antenna measuring equipment .....	44
3.3	Measuring procedure .....	45
3.3.1	Vertical sounding measurement procedure .....	45
3.3.2	Airborne method measurement procedure .....	47
3.3.3	Reference antenna measurement procedure .....	50
3.4	Data presentation .....	52
<b>4</b>	<b>Differences to be expected in practice between calculated and on-site measured performance of VHF and UHF antennas</b> .....	52
4.1	Factors affecting the individual antenna and overall antenna system performance .....	52
4.1.1	Supporting structure .....	52
4.1.2	Significant structures close to the antenna tower .....	52
4.1.3	Climatic factors .....	53
4.2	Comparison of calculated and measured antenna parameters and radiation patterns .....	53

PART 2  
TO ANNEX 1

## Practical aspects of VHF and UHF antennas

### 1 Introduction

The aim of this Part is to describe modern methods of measurement of the radiation pattern of individual antennas and antenna systems. In particular the use of the time domain method appears to be the most accurate and performing approach.

Part 2 also describes the deviations of the radiation patterns encountered in practice from those calculated according to the procedure shown in Part 1.

The way by which a number of factors like the supporting structure, the proximity of other radiating systems, etc. is affecting the overall radiation pattern is also considered.

### 2 Measurement of the characteristics of antenna systems

Measurements are needed to assess the actual individual antenna performance against design data before on-site installation.

In addition is important to evaluate the performance of the individual antennas also when they are assembled together at various azimuthal directions in more complex antenna systems.

#### 2.1 Considerations on the measurement site

The measurement site should be carefully selected since it will affect the accuracy and repeatability of the measurements. In particular the following conditions should be fulfilled:

- absence of interfering sources;
- a suitable distance should be allowed between antenna under test and reference antenna in order to avoid inductive coupling and consequently phase and amplitude distortions;
- a suitable height of the antenna mast should be allowed for proper positioning of the antennas;
- the measurement site should be sufficiently flat to approximate an ideal reflecting or absorbing surface;
- clearance from obstacles causing multiple reflections.

#### 2.2 Parameters to be measured

Normally they are:

- amplitude pattern,
- phase pattern,
- gain,
- impedance matching.

#### 2.3 Methods of measurement

Two basic approaches are used for measuring the performance of antennas: the FDM (frequency domain measurement) and TDM (time domain measurement).

The FDM method is currently used since it does not require expensive measurement equipment. However, the recently developed TDM method allows better performance at increased equipment cost.

##### 2.3.1 The frequency domain measurement (FDM) method

This method uses a transmitting antenna with known characteristics connected to a suitable RF generator. The transmitted signal is received by the antenna under test which can be rotated 360° in the azimuth plane. The amplitude and phase patterns (see § 6.2 of Part 1) can be obtained by comparing the signals received at the various azimuth directions.

The signal received by the antenna under test consists of the direct ray and of a number of reflected rays, depending on the site characteristics, frequency, reference antenna position, radiation pattern side lobes etc.

The true patterns should be determined taking into account only the direct ray. In fact reflected rays affect the resulting measured radiation pattern of the individual antennas so that when they are used to calculate more complex antenna systems significant deviations between the calculated and measured antenna system pattern are to be expected. These deviations may be considerable particularly when minima and side-lobes are to be evaluated.

The gain is usually measured by the absolute method paying attention to carefully control the effects of the reflected rays.

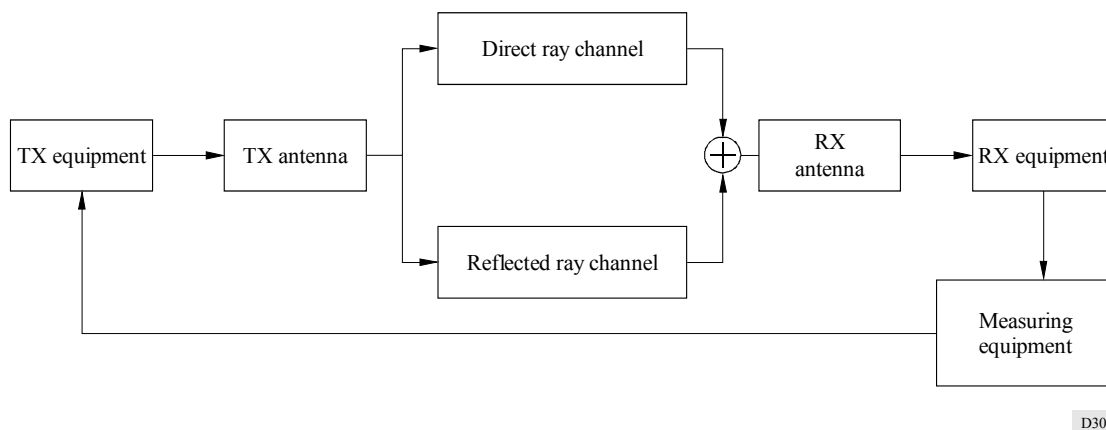
### 2.3.2 Time domain measurement (TDM) method

Amplitude and phase pattern measurements can be performed with definitely better accuracy when using the TDM method since the effects of reflected rays can be almost completely removed from the measurement procedure.

This improvement is based on the use of the direct and inverse Fourier transform associated to an analytical gating process.

The complete system layout (including measuring equipment and the antenna) is shown in Fig. 30.

FIGURE 30  
Block diagram of TDM method



D30

Since the time-domain voltage output to a pulse input voltage is, by definition, the Fourier transform of the system transfer function, the frequency response of the system (in the presence of two propagation paths) can be determined by using a spectrum analyser or similar instruments.

By performing the inverse Fourier transform of the frequency response, the time-domain response, containing both the direct and the reflected path components, can be obtained. These contributions can be separated in the time domain due to their different path lengths. The input pulse width should be optimized according to the type of the individual antenna under test, bearing in mind that shorter pulses will allow for more accurate discrimination.

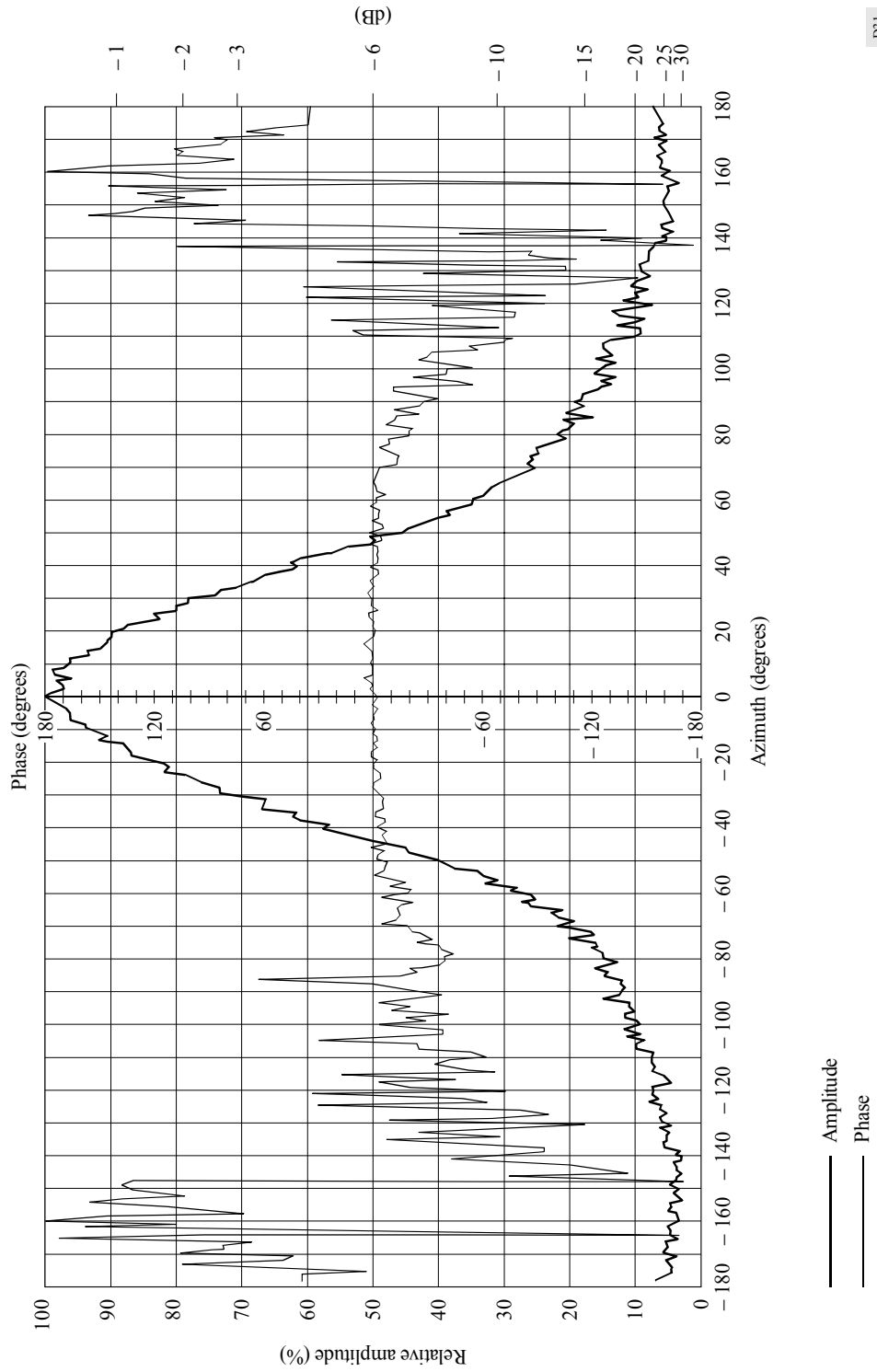
The analytical gating process improves discrimination by removing unwanted time-domain responses. It can be applied to the various time-domain components in order to get the frequency response of the direct or the reflected path component.

Since the channel characteristic is linear, the frequency responses of the two path components differ only by an attenuation factor in the case of the amplitude response and by a linear phase shift in the case of the phase response.

However, the reflections due to mismatch between the transmitter and its antenna as well as between the receiver and its antenna will have to be kept at acceptable levels by using high quality cables and connectors. Rotary joints should be avoided.

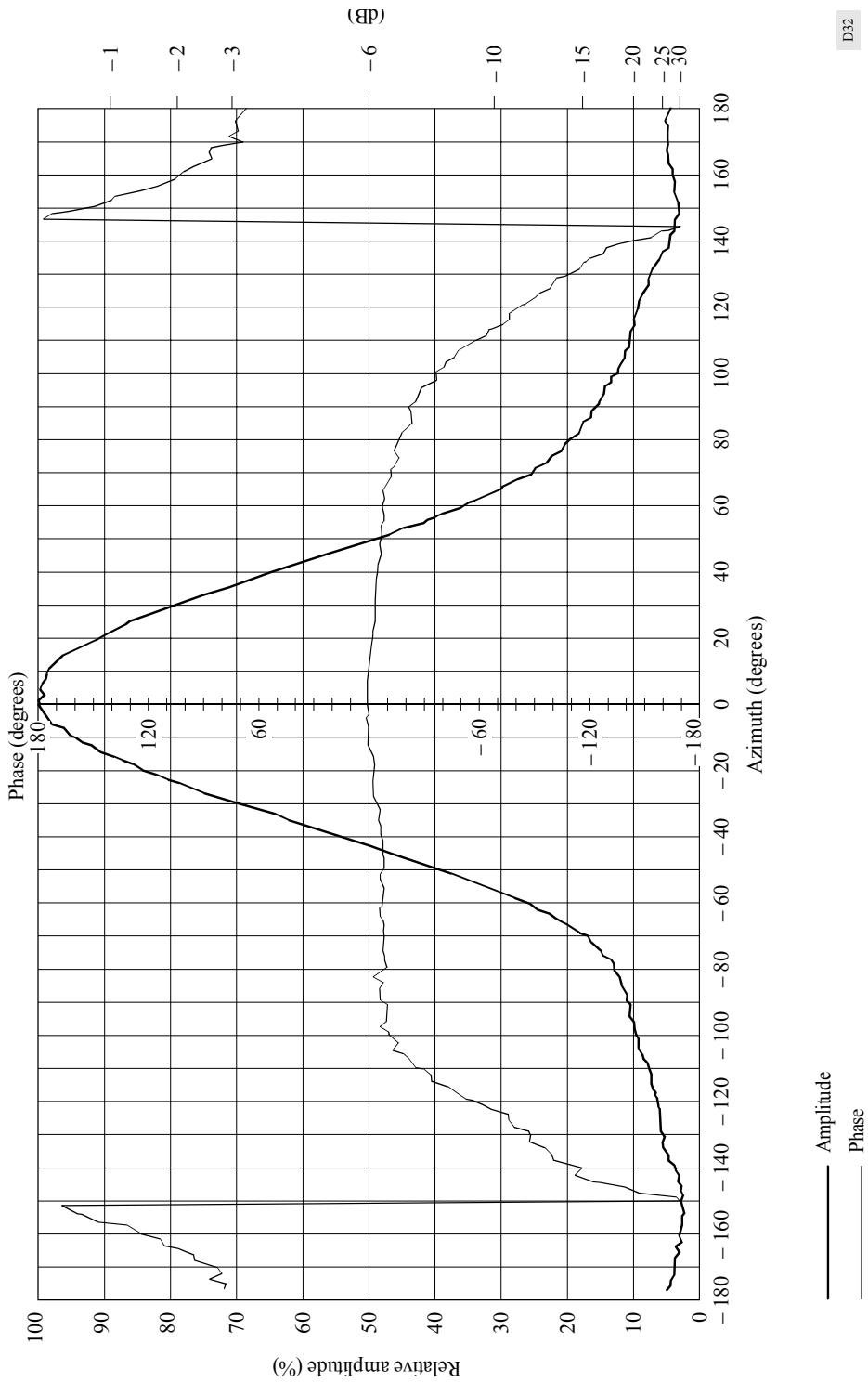
Figures 31 and 32 show examples of amplitude and phase patterns when using or not using the time domain method.

FIGURE 31  
Amplitude and phase patterns when not using time domain measurement



D31

FIGURE 32  
Amplitude and phase patterns when using time domain measurement



D32

## 2.4 Measuring equipment

The measuring system consists of a power RF generator with a level sufficient to provide a suitable  $S/N$  ratio, a field strength meter and a vector voltmeter to determine the phase centre. The use of more sophisticated computer-controlled measuring tools like a spectrum analyser or a network analyser is recommended.

## 2.5 Measuring procedures

Measuring procedures may vary according to the parameters to be measured and to the available instruments. In any case, the following conditions have to be satisfied:

- inductive coupling between antennas is to be minimized, i.e. the distance  $R$  between the antennas should be greater than  $10 \lambda$ . This will ensure a near to far field amplitude ratio of at least 36 dB;
- the phase distortion in the incident wave plane is also to be minimized in order to achieve good minimum discrimination. Phase distortion therefore should not be greater than  $\pi/8$  or  $R > 2 D^2/\lambda$ ;
- the transmitting antenna beamwidth should allow for amplitude variations of the emitted wavefront in the direction of the antenna under test not greater than 0.25 dB;
- the antenna height should be selected in order to minimize the interception of the measurement site ground by the transmitting antenna main lobe. The amplitude of reflected rays can therefore be reduced. A recommended practice is to select an antenna height that results in positioning the first null of the transmitting antenna vertical pattern in the direction of the base of the tower.

When impedance matching measurements are to be carried out the antenna position should be suitably selected to avoid inductive coupling and reflections against from obstacles. In general the antenna main lobe should be pointing upwards so that the effective reflected and transmitted power can be more easily measured.

In the FDM method a sinusoidal test signal is used having a frequency within the antenna's operating frequency band. A series of measurements of the signal at the RX antenna is then performed at various frequencies with a predefined angular step. The measured amplitude values are then normalized to the maximum to obtain relative attenuation values expressed in dB. The measured phase values will be expressed as phase differences with respect to the reference angle. In the TDM method a pulse test signal with a suitable duration is used. The radiation pattern can be obtained using the values obtained from the frequency response of the pulse signal "cleaned" all over the angular sector.

Both the amplitude and the phase patterns for use in pattern calculations are normally determined.

The antenna gain is measured by using two identical devices as transmitting and receiving antenna placed at the same height and oriented in the maximum power transfer conditions. In this case when the vertical sounding method is used in the FDM mode, a suitable common antenna height should be selected at each test frequency in order to allow for an easy determination of the direct ray.

Also in TDM the two antennas are oriented in the maximum power transfer condition. Since the reflected ray can be cancelled, the antenna position needs not to be changed as in the FDM. Impedance matching is measured as the ratio between transmitted and reflected power by means of a directional coupler.

Currently available advanced measuring systems allow to transfer the reference plane at the antenna input, avoiding errors due to the measuring equipment. The TDM method gives the possibility of determining any mismatching present in the measuring equipment.

## 2.6 Data presentation

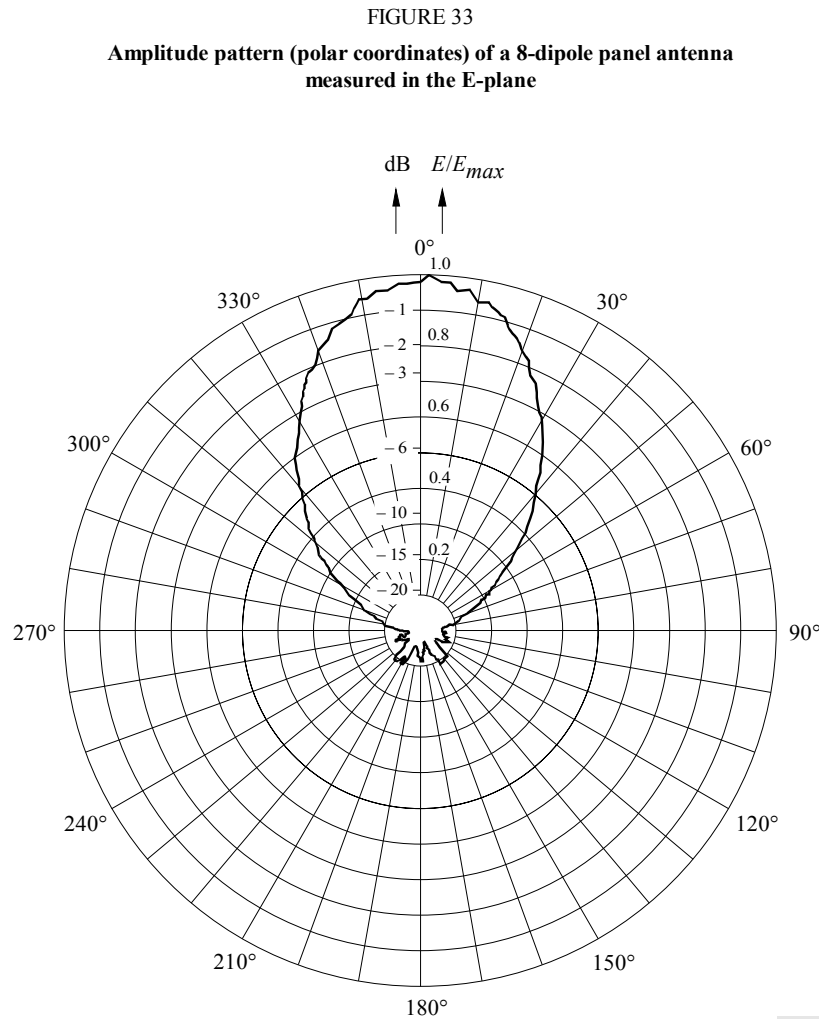
The plane containing the elements of the antenna is taken as the reference plane for antenna pattern presentation.

The amplitude pattern in the reference plane and in the corresponding orthogonal one should be represented in Cartesian and polar form. The phase pattern should be represented only in Cartesian form.

Gain and impedance matching data should be presented in Cartesian form.

Figures 33 to 38 give some examples of the resulting amplitude and phase patterns in the two planes, both in polar and Cartesian form.

A linear scale is used with values expressed both in percentage and in dB.



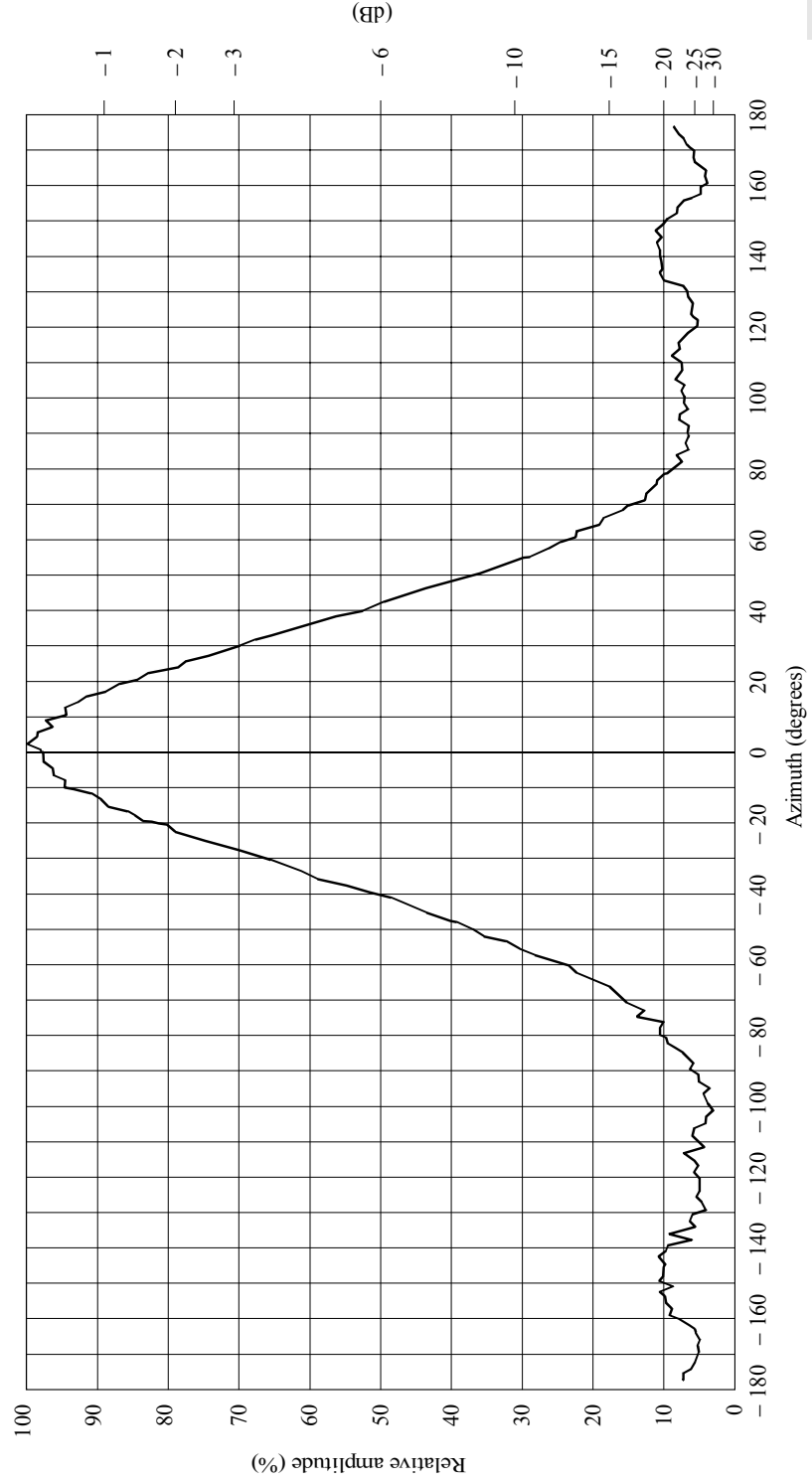
### 3 On-site measurements of the antenna system characteristics

Since the efficiency of a radio system depends mainly on its antenna, the radiation patterns and gain need to be determined with sufficient accuracy. When the radiation pattern of complex antenna systems is affected by a number of uncontrollable factors in its operating environment, it can only be determined by on-site measurements.

#### 3.1 Methods of measurement

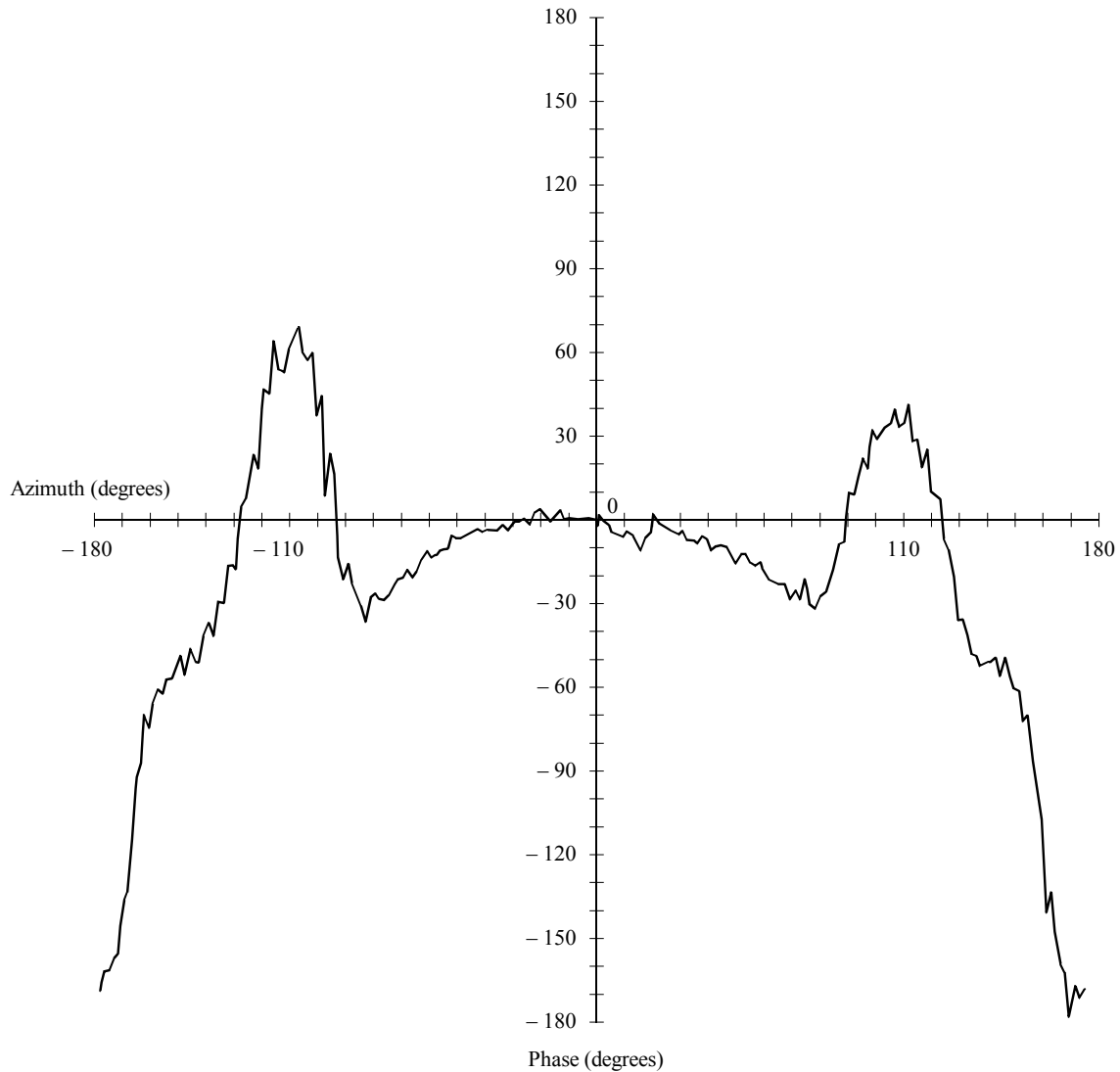
Three main methods of on-site measurements of antenna characteristics are described. Although in principle any method can be utilized, the actual choice will depend on the system economy, set-up complexity, necessary equipment and measurement time. For example, the airborne method is more expensive than any other method but measurements can be carried out in a short time on several antenna systems on the same tower or located nearby. On the contrary, more economical terrestrial methods generally need more time to provide the same results and sometimes due to environmental constraints reliable measurements cannot even be performed.

FIGURE 34  
Amplitude pattern (Cartesian coordinates) of a 8-dipole panel antenna measured in the E-plane



D34

FIGURE 35  
Phase pattern (polar coordinates) of a 8-dipole panel antenna measured in the E-plane



D35

### 3.1.1 Vertical sounding method

This method requires a special particular van equipped with an antenna on a mast that can be raised on the vertical of the measurement point to evaluate electromagnetic field variations as a function of the height above the ground.

The measurement will provide an interference pattern resulting from the combination of the direct and reflected rays. When only one reflected ray is present, this pattern is represented by a cosinusoidal function having its first maximum at a height  $h = \lambda d / 4H$ , where:

$\lambda$ : wavelength

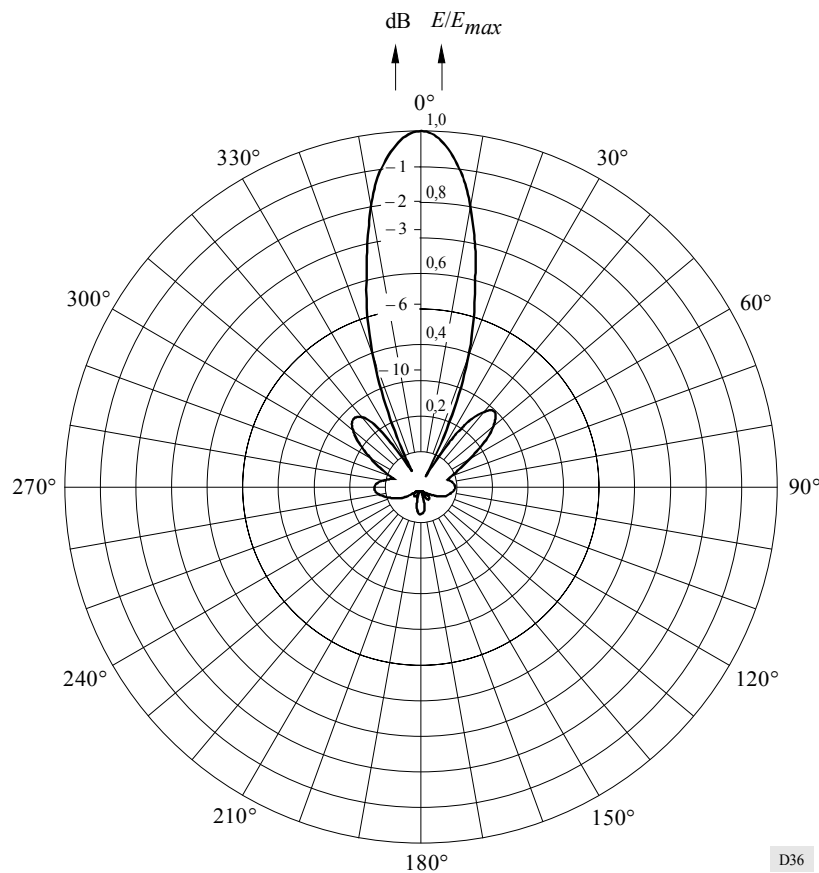
$d$ : distance from the transmitter and receiving antenna

$H$ : relative height of the transmitter antenna with respect to the measuring point.

In these conditions the electromagnetic field in free-space propagation conditions can easily be determined and its value can then be compared with the corresponding theoretical one (calculated according to Recommendation ITU-R P.525) to assess the overall antenna's performance. In general, measurement points showing an interference pattern with large variations with respect to the theoretical function should be discarded. However, if suitable measuring points cannot be found due to environmental constraints, alternative methodologies should be considered.

FIGURE 36

**Diagramme des amplitudes (coordonnées polaires) d'une antenne-panneau de 8 doublets, mesuré dans le plan H**

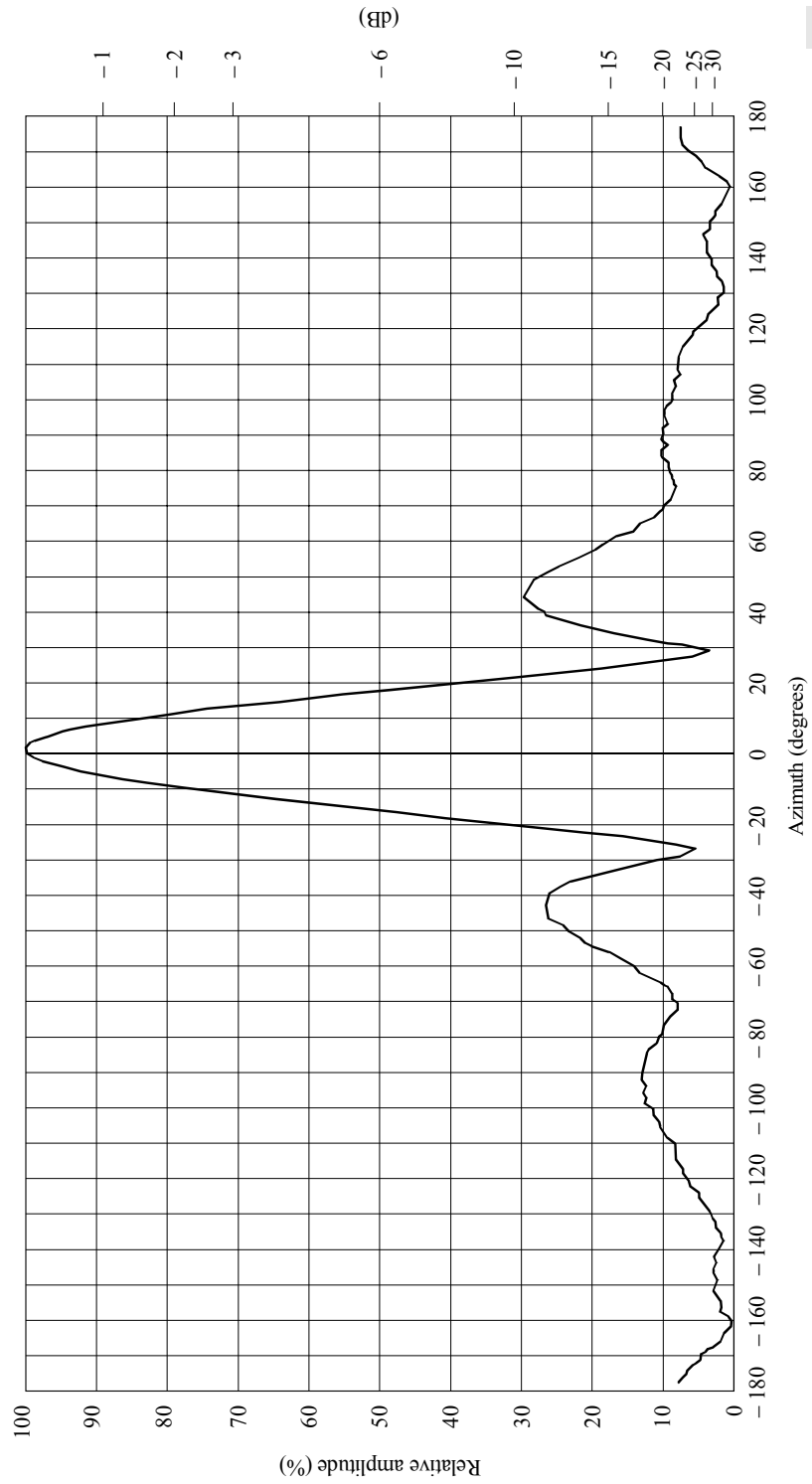


D36

### 3.1.2 Airborne method

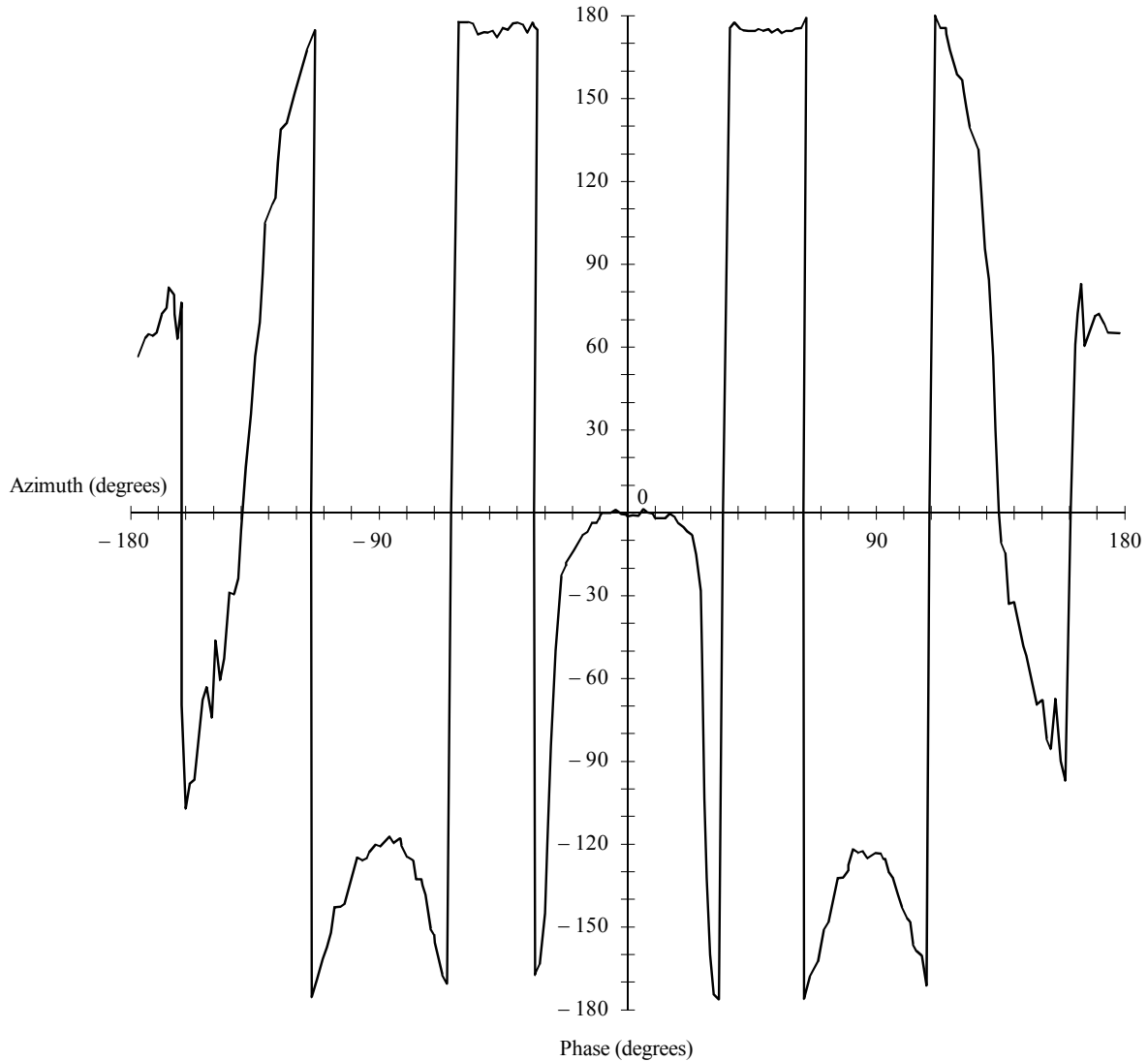
This method based on an airborne measuring equipment, is considered to give the most accurate and reliable results when the gain, and the horizontal and vertical radiation patterns of an antenna are to be evaluated. In this case, the measuring receiver is mounted on a helicopter (the preferred type of aircraft for these measurements), while the antenna under test is operated in transmission mode. In some cases, particularly when measuring pattern nulls, a rather high transmitter power may be required to ensure a sufficient signal-to-interference ratio at the receiver.

FIGURE 37  
 Amplitude pattern (Cartesian coordinates) of a 8-dipole panel antenna measured in the H-plane



D37

FIGURE 38  
Phase pattern (polar coordinates) of a 8-dipole panel  
antenna measured in the H-plane



D38

### 3.1.3 Reference antenna method

This method is based on the use of a reference antenna with known characteristics. The reference antenna is mounted as close as possible to the antenna to be measured and fed with a signal having possibly the same operating frequency. By comparison of the measured field strengths generated by both antennas at the same point, the radiation pattern of the antenna under test can be determined. The effect of the terrain on the receiving field strength is therefore eliminated.

## 3.2 Measuring equipment

### 3.2.1 Vertical sounding measuring equipment

The following equipment is installed on a specially equipped van, with independent electric power supply generator:

- a retractable mast able to be raised up to intercept the first maximum of the field strength intensity (see also § 3.3.1) connected through a suitable interface to the computer that will acquire elevation and azimuth of the receiving antenna on the mast;
- a suitable test receiver with:
  - high dynamic range,
  - good electromagnetic compatibility,
  - ruggedness and stability when subject to vibrations and temperature variations,
- a receiving antenna to be installed on the mast,
- a positioning system such as a global positioning system (GPS),
- a control computer connected to the positioning system and the interface of the mast, to process the measured data.

### 3.2.2 Airborne measuring equipment

A radiation pattern measuring system may include the following components:

- a test receiver (able to be controlled in scan mode) with:
  - high dynamic range,
  - good electromagnetic compatibility (EMC),
  - high ruggedness and stability (with respect to vibrations and temperature variations in the helicopter),
- a receiving antenna (test probe) mounted in such a manner that the influence of the helicopter on the radiation pattern of the receiving antenna is reduced to a minimum. This can be achieved with a mast which can be lowered at least 3 m below the helicopter;
- a positioning system such as the GPS using an airborne and a ground-based receiver plus an accurate altimeter;
- an airborne control computer with peripheral data processing equipment.

Figure 41 shows a simplified block diagram of the equipment.

The ground based reference (GPS) receivers are used to enable differential GPS which gives very high accuracy. However, although GPS is the most advanced system for determining the position during the flight, other systems providing suitable accuracy might be used.

The data processing equipment includes a computer and a pattern plotting peripheral.

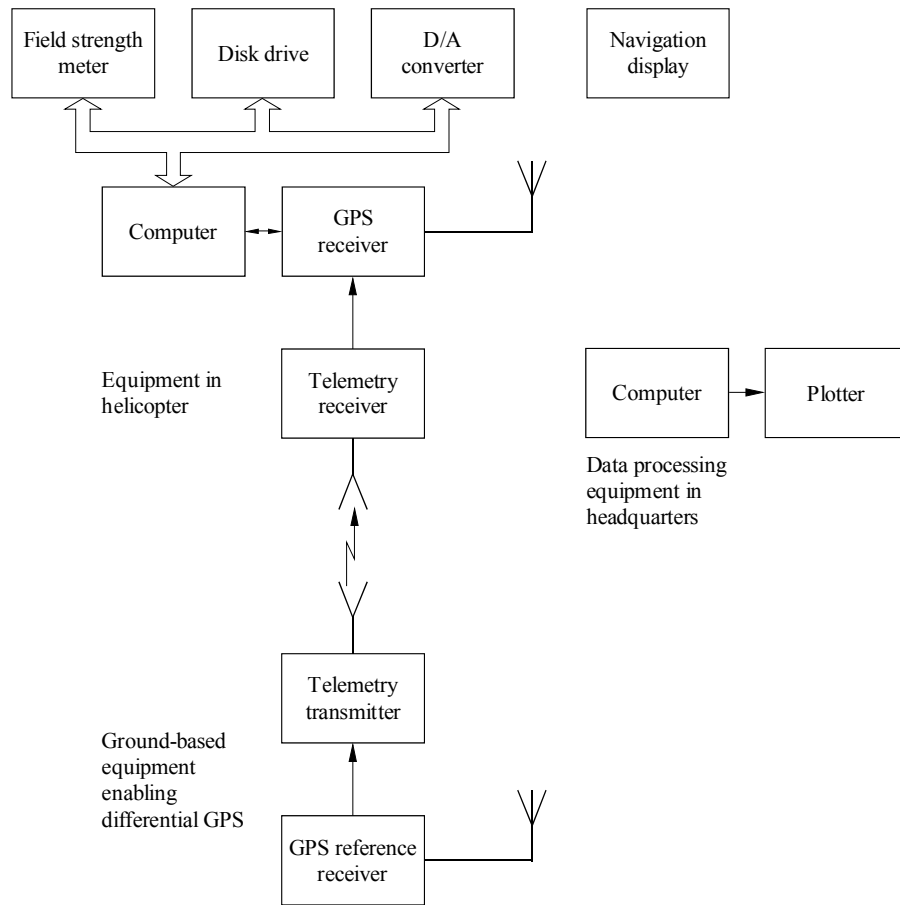
At the transmitting side a signal source having a stable and calibrated output power level is needed. This source could be the normal transmitter.

### 3.2.3 Reference antenna measuring equipment

It may include the following components:

- one or two test receivers, depending on the desired measurement procedure, with:
  - high dynamic range,
  - high electromagnetic compatibility (EMC),
  - high ruggedness and stability (with respect to vibrations and temperature variations in the van),
- a receiving antenna mounted on the roof of the van (log-periodic or turnstile antenna, according to the selected procedure),
- a control computer with peripheral data processing equipment installed in the van,
- a positioning system,
- a reference antenna with calibrated radiation pattern,
- a portable battery-operated field-strength meter.

FIGURE 39  
Block diagram of the measuring equipment



D39

### 3.3 Measuring procedure

#### 3.3.1 Vertical sounding measurement procedure

A preliminary transmitting and receiving antenna data entry procedure is required before the actual measurements can be carried out.

The following transmitting antenna data are to be entered:

- name and site of the transmitting station,
- geographical coordinates,
- frequency and polarization of the emission,
- e.r.p. maximum (dBK),
- height of the antenna above sea level,
- theoretical vertical diagram (to be possibly corrected against the measured one).

The following receiving antenna data are to be entered:

- gain,
- cable attenuation.

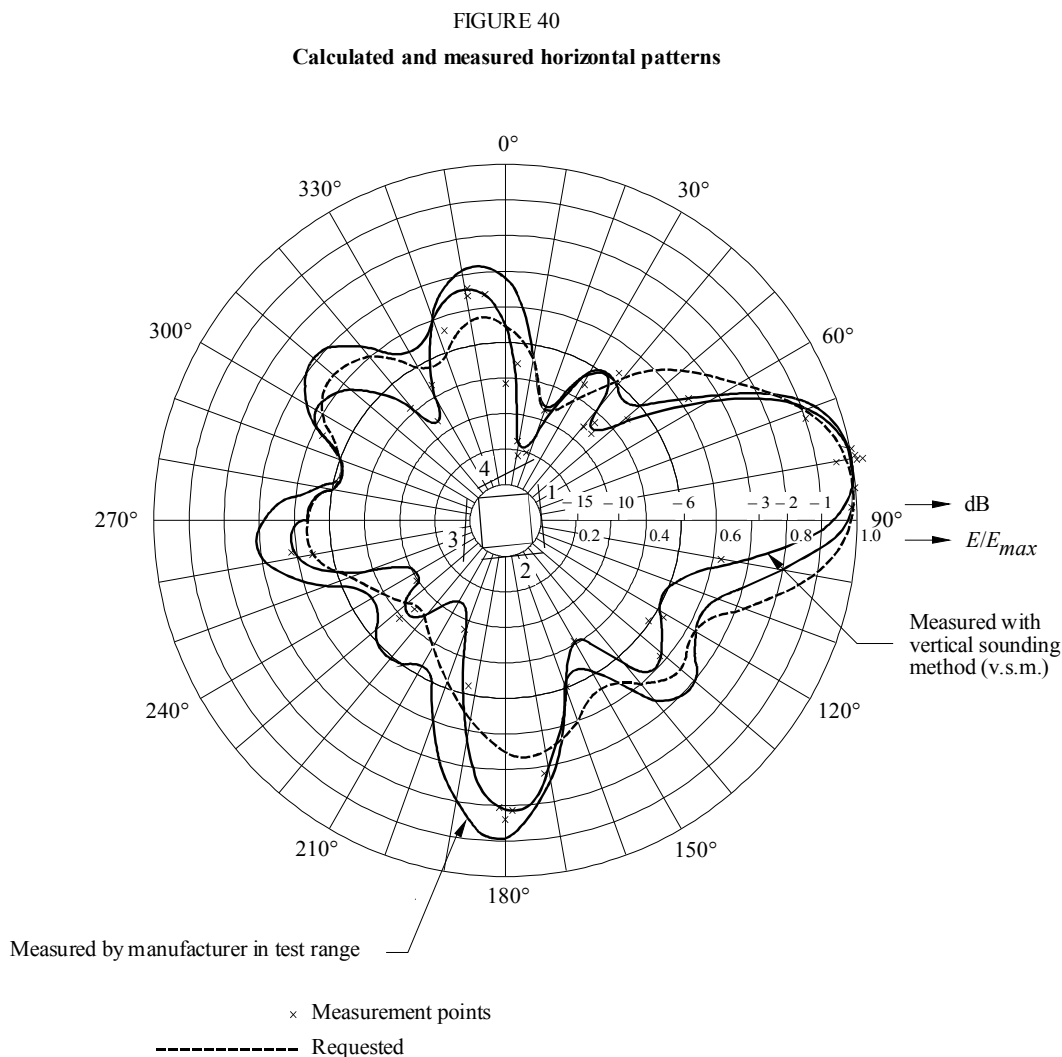
When a suitable measurement point has been selected, the relevant geographical data such as the site name, height above sea level and associated coordinates (as possibly acquired by the GPS) are entered.

The above data are suitably processed to obtain distance, azimuth and zenith angles of the selected measurement point with respect to the transmitter, and the corresponding value of the theoretical relative amplitude vertical radiation pattern.

When the receiving antenna has been correctly oriented in the direction of the transmitter, the mast is raised and a received voltage sample is acquired at regular elevation steps (of typically 20 cm). All the voltage data values are then suitably stored and processed to obtain the typical interference pattern. This pattern will subsequently be analysed for calculating the direct field.

### 3.3.1.1 Data processing

After a suitable input data validation procedure is performed, the accepted values are further processed to obtain a series of relative values  $E/E_{max}$ , where  $E_{max}$  is the maximum value measured in correspondence to the main lobe. These data are then plotted in a polar diagram and compared to the theoretical vertical pattern (see Fig. 40).



D40

### 3.3.1.2 Considerations on the practical implementation of the vertical sounding method

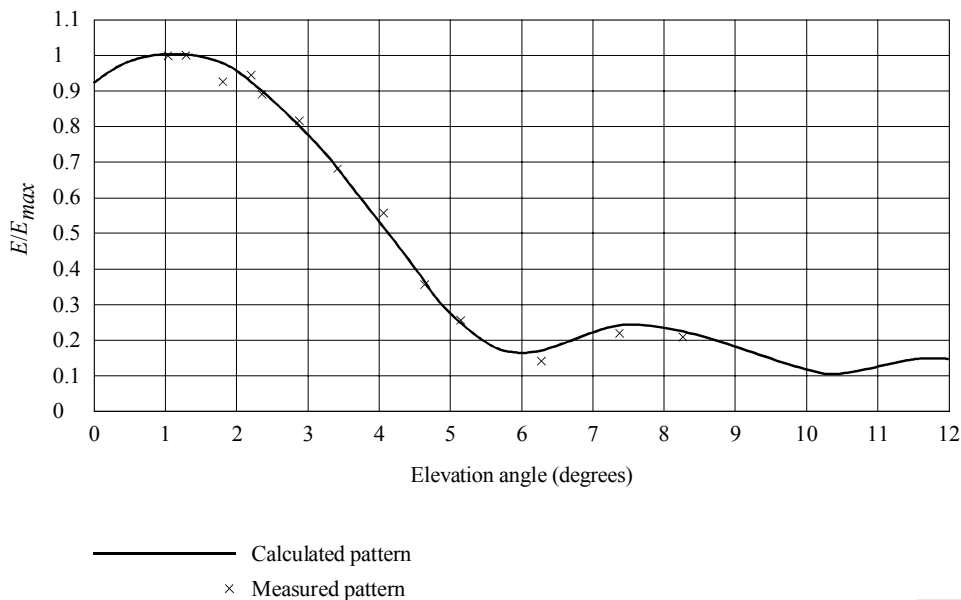
Before the actual measurements can be performed, a suitable analysis of the environment near the antenna under test is to be carried out, bearing in mind that all the measurement points have to be selected along roads that can be accessed by the test van.

A digitized terrain map (DTM) with a suitable software procedure to derive the terrain profile from the antenna site to the measurement point is recommended. In fact by the terrain profile it can more easily be evaluated the line-of-sight propagation conditions of the selected measurement point with respect to the transmitting antenna.

Since the measured horizontal pattern values are to be referred to the measured maximum value of the vertical pattern, this last pattern has to be firstly determined.

A typical situation is represented by an antenna system on a square section supporting structure having different individual antennas mounted on each side. This arrangement requires to perform a series of different measurements in points selected in each angular sector covered by the individual antenna. In this case a first suitable point is selected in the relevant sector. The vertical pattern measurement is initiated from this point in order to obtain a diagram showing the relative variation of the e.m. field with respect to its maximum value. The diagram shown in Fig. 41 refers to a typical case where the transmitting antenna is installed on the top of a hill above the service area.

FIGURE 41  
Calculated and measured vertical patterns



D41

The horizontal radiation pattern measurement is performed after the vertical pattern. Since in the interference pattern the height of the first maximum of the received field is given by  $h = \lambda d / 4H$  (see § 3.1.1), the retractable height  $h$  of the mast has to be carefully selected. The actual value should result from a suitable compromise between its maximum determined by mechanical considerations and its minimum determined by the tilt angle which can affect the maximum value to which the vertical pattern relative values are referred.

At VHF a good compromise value may be difficult to achieve since the vertical pattern variations may considerably affect the measurements of the horizontal pattern.

In addition, in the directions where the measured value results from two individual antennas having different vertical radiation patterns like in the crossover directions, the dominant contribution cannot be easily identified. In these cases a possible solution may consist in selecting a measuring point at a distance  $d$  where the depression angle results in about the same value for both vertical radiation patterns. In any case the final evaluation of the direct e.m. field remains within the operator, who examining the shape of the interference pattern has to discard measured values showing large differences with respect to the theoretical function.

### 3.3.2 Airborne method measurement procedure

A set of measured radiation patterns normally consists of one horizontal radiation pattern (HRP) measured at the elevation angle of the maximum radiation and five vertical radiation patterns (VRPs) measured at each frequency in specific directions at an elevation angle varying from  $-15^\circ$  to  $+3^\circ$ .

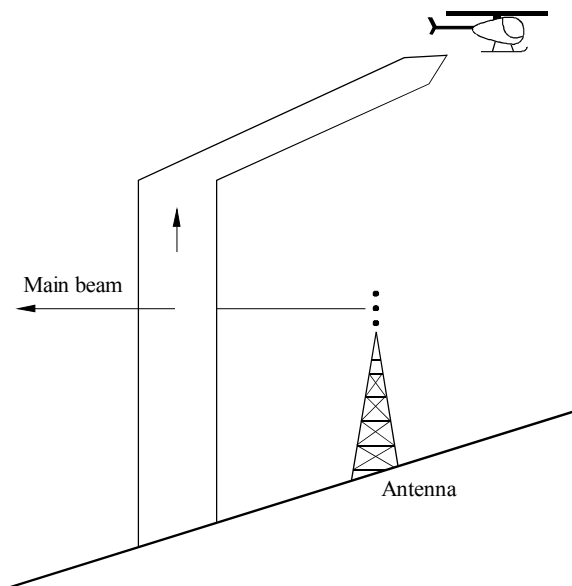
A careful preparation is needed before the actual measurements can take place. Both the airborne and the ground equipment must be checked to verify their proper operation. The test signal generator (or the normal transmitter) feeding the antenna under test has to be set to its calibrated power value.

After the aircraft take-off, the position determining equipment (GPS) operation is checked and, if necessary, the coordinates of the antenna under test are determined and entered in the computer as origin of the measured coordinate system.

During the measuring flight the helicopter should follow predetermined routes, as is described below. The actual flight paths are recorded using the output from the GPS which by means of suitable computer processing, gives the actual position of the helicopter with respect to the antenna being measured. This helicopter position information is also presented in real-time to the pilot, helping to maintain a correct flight path.

Vertical measurements are made by a combination of vertical climbing and approach flights. The helicopter starts the measurements close to the ground at an appropriate distance, depending on the type of antenna under test. It will then climb to an altitude corresponding to the wanted maximum elevation angle. If the complete vertical pattern up to zenith is of interest, the helicopter follows an approach course over the antenna after reaching an altitude of approximately 1 000 m ( $20^\circ$ ) (see Fig. 42).

FIGURE 42  
Vertical flight path



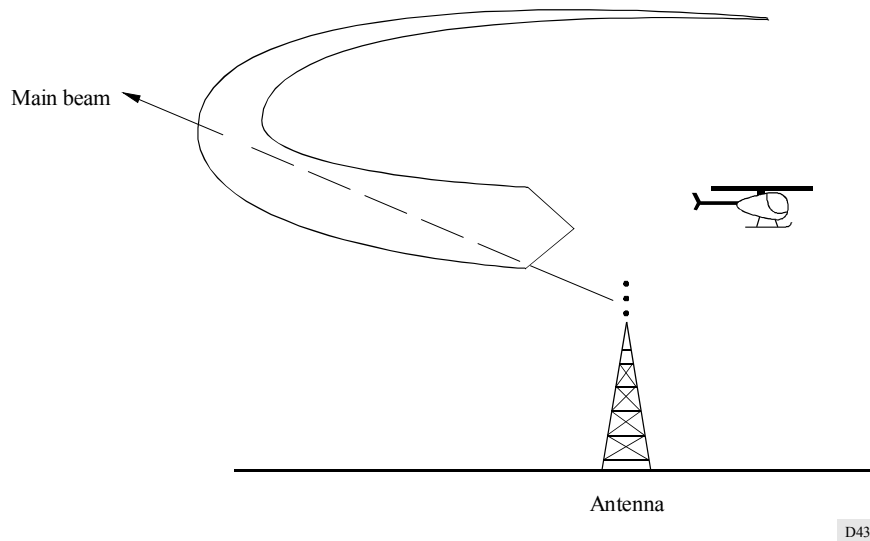
The results of the vertical measurements include the value of the elevation angle at maximum gain (i.e. the main lobe maximum) at which the horizontal diagram should be measured. At this elevation angle the helicopter flies in a circle around the antenna at a radius depending on the type of antenna under test (see Fig. 43). For this flight path it is very important that the correct elevation angle is accurately maintained since compensation for any deviation is difficult.

The distances for both VRP and HRP measurements should be determined before each measurement (see § 3.3.2.2).

The received field strength intensity is measured by the airborne test receiver (or field strength meter). At the same time the airborne computer is receiving position updates from the GPS. The position data is then used to convert the measured input signal levels into field strength values at a normalized distance taking into account the characteristics of the receiving antenna.

The test receiver should carry out measurements in an averaging mode, i.e. each signal level sample will consist of an average of the received signals in a time interval of 100 ms in order to eliminate the modulation effects. The test receiver should be able to be operated in a scanning mode in order to facilitate measurements on at least three frequencies on the same measuring flight path. Furthermore, the measuring system should allow to acquire at least two samples per degree in the horizontal plane and at least five samples per degree in the vertical plane. These samples are to be stored together with their corresponding position data.

FIGURE 43  
Horizontal flight path



The measured values are displayed on a screen in the form of an antenna pattern, in order to allow the on-board operator to verify the proper operation of the measurement system during the flight.

### 3.3.2.1 Processing the measured data

When the airborne measurements have been completed, the measured data is analysed and the patterns are calculated and plotted. In this analysis, the samples of signal level are converted into field strength values at a normalized distance taking into account the characteristics of the receiving antenna and the position information. All obviously erroneous samples are discarded.

The e.r.p. in a given direction is then calculated from the field strength and its corresponding distance. Normally the plotted diagrams are expressed as relative to the e.r.p. in the maximum radiating direction.

The gain of the antenna is calculated as the ratio:

$$G_d = \frac{e.r.p.}{P_{in}}$$

where  $P_{in}$  is the power fed to the antenna.

### 3.3.2.2 Considerations when using the airborne (helicopter) method

When measuring VHF/UHF antennas the ground effects should be kept to a minimum.

Figure 44 shows how to select the measuring distance in order to minimize reflections at a given antenna height. Shorter distances result in wider angles at the reflection point that will reduce the reflected energy. Therefore, the selected distance should be as short as possible but enough to be in far field conditions. Furthermore, the receiving antenna should be directional and steerable in order to be continuously oriented towards the antenna under test.

A formula generally used to calculate the minimum measuring distance with sufficient accuracy to be in far field conditions, is:

$$d = \frac{2h^2}{\lambda}$$

where:

- $d$ : measuring distance (m)
- $h$ : aperture (m) of the antenna
- $\lambda$ : wavelength (m).

In practice a typical measuring distance of 2 000-2 500 m is generally used.

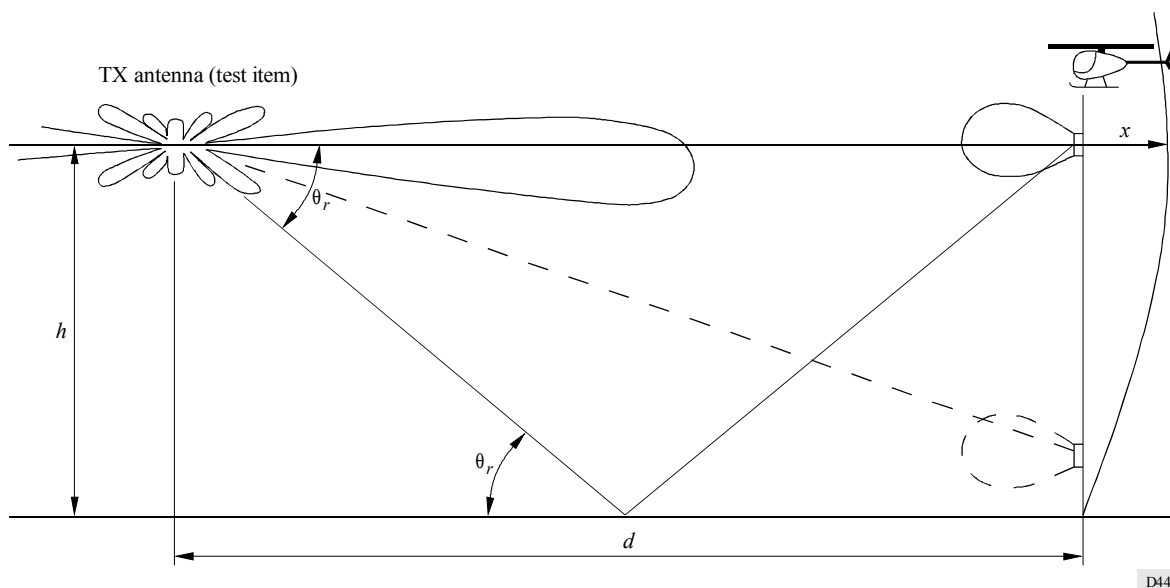
The accuracy of the results depends on the performance of the equipment used to measure the field strength and location. Therefore careful consideration has to be given to the following factors:

- the receiving antenna characteristics and its mounting on the helicopter;
- the test receiver (field strength meter), including the cables;
- the position determining system used to get the true three dimensional coordinates and to assist the pilot.

When GPS is used, the error in the recorded two dimensional position of the helicopter is in the order of 5 m. This error will result in a position error less than 0.5 dB.

A critical point is to maintain correct altitude in the horizontal flight path. When measuring a high gain UHF antenna, a vertical angle deviation of  $0.3^\circ$  (as seen from the antenna under test) may result in an error of 0.5 dB. Therefore, at shorter distances it will be more difficult to maintain the correct altitude. For a suitable reliability of the horizontal flight path measurements, the HRP should be measured at least twice in order to get meaningful results.

FIGURE 44  
Representation of flight path



### 3.3.3 Reference antenna measurement procedure

The measurement of vertical pattern with a reference antenna should be done starting from the horizontal pattern maxima. The measurement of horizontal pattern can only be done starting from the vertical pattern maximum. A number of environmental factors such as thick forest and vegetation can affect the measurements carried out by means of a normal field-strength meter since they result in a time fluctuation of the measured field strength. To achieve meaningful results, measured data should possibly be integrated over a time interval of some minutes.

Two different measurement procedures can be implemented:

- point-to-point field strength measurements by a field-strength meter and a log-periodic measuring antenna placed 50 cm above the ground;
- simultaneous, continuous recording of both field strengths with two field-strength meters connected to a suitable recorder in the test van. A typical measuring turnstile antenna 0.7 m mounted on the vehicle roof and placed 3.2 m above the terrain is used.

End-to-end measurements by means of reference antenna with continuous field strength recording, are usually providing good results even when the transmitter is not in line-of-sight.

Distance measurements require a certain time to convert the recorded field strength values to the selected coordinate system (i.e. to determine the elevation angle as a function of the distance to transmitter and height over sea level). In addition it may result practically impossible to maintain a tolerance of about  $\pm 3^\circ$  in the radial direction from the transmitter while running on roads that can be accessed by the test van.

Although point-to-point measurements are less sophisticated, they provide results comparable with end-to-end measurements only under conditions of line-of-sight propagation and terrain clearance. In these conditions by means of a simple portable, battery-operated field strength meter it is possible to freely move in the measuring area without depending on existing and available roads.

Since the power radiated at smaller elevation angles does not reach the ground, it is generally possible to select the measuring point distance that results in a "clean" pattern. Although some measuring points will have to be discarded due to unfavourable terrain conditions (vegetation or inaccessible terrain), the position and depth of minima can in general be determined with sufficient accuracy.

### 3.3.3.1 Processing the measured data

The curve shapes of measured patterns could be plotted on the bases of continuously/point-to-point recorded field strength.

The drawn radiation patterns are absolute diagrams giving the effective radiated power e.r.p. as a function of the elevation angle, if the radiated power of the reference radiator is precisely known.

When using an end-to-end measurement technique, with a distance resolution of about 200 m distances and trinomial equalization based on sliding averages, the random fluctuations are eliminated and the real form of vertical pattern becomes evident. Due to the great number of measured values, the accuracy at smaller elevation angles is higher than at large angles. Therefore, at elevation angles  $> 3^\circ$ , measurements should be performed with a distance resolution of  $< 200$  m in order to get a sufficient number of test points.

Experience with end-to-end measurements on test vans showed that reliable pattern measurements by reference antenna demand for a very large set of measured values to perform suitable statistic evaluation and to achieve a sufficient smoothing of the radiation pattern.

When due to heavy reflections, large variance takes place and no stable median value can be found, the test point becomes useless. These points are identified by reflected signal coming from different directions that do not correspond to the direction of transmitter.

The individual test points at each elevation angle may have distances ranging from few metres to even some 100 m depending of local conditions. It is therefore important to determine the elevation angle with a tolerance of less than about  $+0.05^\circ$  and an azimuth of about  $+2.5^\circ$ .

The evaluation of the measured results, i.e. the determination of the median value, of the corresponding elevation angle and the pattern plot needs to be done at the measuring position. Only in that way it can be assessed whether the measuring values are sufficient to plot the pattern or further test points are needed.

### 3.3.3.2 Considerations when using reference antenna method

Some caution is recommended when the elevation angle of the test point is determined by its distance and relative height. While the distance from the transmitter can be accurately determined from the maps, the height above sea level can often not be precisely determined, especially in hilly terrain. At small distances to the transmitter considerable angular errors can be introduced. The use of a barometric altimeter may improve the situation. In the case of transmitter visibility the elevation angle can be measured directly with a theodolite.

Additional information can also be drawn from the results of measurement procedures using a reference antenna, since not only radiation characteristics in free-space conditions are of interest, but also the improvement in received field strength when using a directional transmitting antenna.

This increased gain, sometimes called operational gain, gives the increase in the energy received at any receiving position when an antenna having a directivity higher than the reference antenna is used. The median of operational loss was shown to differ about +1 dB with respect to free space gain and about +2 dB on irregular terrain. Antennas with low centre height, installed on mountains have an operational gain of more than 2 dB lower than that of free space.

Thus the measurement by means of reference radiator provides radiation characteristics of transmitting antenna system considering terrain characteristics of the service area. Unlike during helicopter measurements the free-space pattern is measured.

### 3.4 Data presentation

With reference to azimuthal and zenithal plane, it is suggested to present the horizontal amplitude pattern in polar form and the vertical amplitude pattern in Cartesian form.

## 4 Differences to be expected in practice between calculated and on-site measured performance of VHF and UHF antennas

The comparison of calculated and measured radiation patterns allows to highlight the influence of factors not taken into account in the calculation. Some significant factors are described below.

### 4.1 Factors affecting the individual antenna and overall antenna system performance

#### 4.1.1 Supporting structure

The following factors will affect the antenna system performance:

- mutual coupling between the individual antennas will modify the amplitude and phase of their feed current. The resulting radiation pattern will therefore be different from the calculated one;
- the metallic lattice supporting structure is likely to work as a parasitic slot-antenna, in particular if dimensions are close to resonance;
- side offset is useful to obtain stable performance with regard to matching. However, such offset should be limited if it leads to a screening of adjacent individual antennas;
- since the reflector of the majority of directional individual antennas has a limited size, also the supporting structure behind the individual antenna will to some extent act as a secondary reflector.

In case of offset along the supporting structure side, this secondary reflector will be asymmetrical with regard to the radiator and the pattern will be skewed.

Similar effects will occur in all cases of asymmetrical mounting on a tower;

- other antenna systems on the same tower, platforms, stays, ladders, bad lay-out of the distribution feeder cables, etc. might also influence the performance – usually in an unpredictable way.

#### 4.1.2 Significant structures close to the antenna tower

The factors affecting antenna systems may result from natural environment and man-made structures.

The environment affects the diagram shape in a permanent and uniform manner according to the natural characteristics of the site.

Structures close to the antenna tower, on the other hand, modify the radiation pattern in particular directions, depending on the distance and their physical characteristics. The resulting effect may be of considerable importance depending on the number and size of the nearby structures.

The above factors may differently affect the performance of individual antennas and more complex antenna systems. Such a difference is due to coupling effects and to the attenuation and, in general, to a combination of both. According to the prevailing influence of the above effects, the performance at VHF and UHF bands may be quite different.

### 4.1.3 Climatic factors

Heating by the sun will result in bending the supporting structure and overall beamtilt variation.

Yagi antennas are very sensitive to icing. This phenomenon in extreme cases may result in inversion of the front-to-back ratio. Impedance mismatch will increase for all antenna types during icing conditions.

## 4.2 Comparison of calculated and measured antenna parameters and radiation patterns

The expected difference between calculated and measured radiation patterns may range from some tenths of dBs to some tens of dBs.

This difference may be more important particularly in proximity of pattern nulls and side lobes. When the coupling effects prevail, larger differences can be expected at VHF than at UHF. On the contrary, if the attenuation effect prevails, larger differences are to be expected at UHF. In addition, the effect of these variations will depend also upon the complexity of the antenna system.

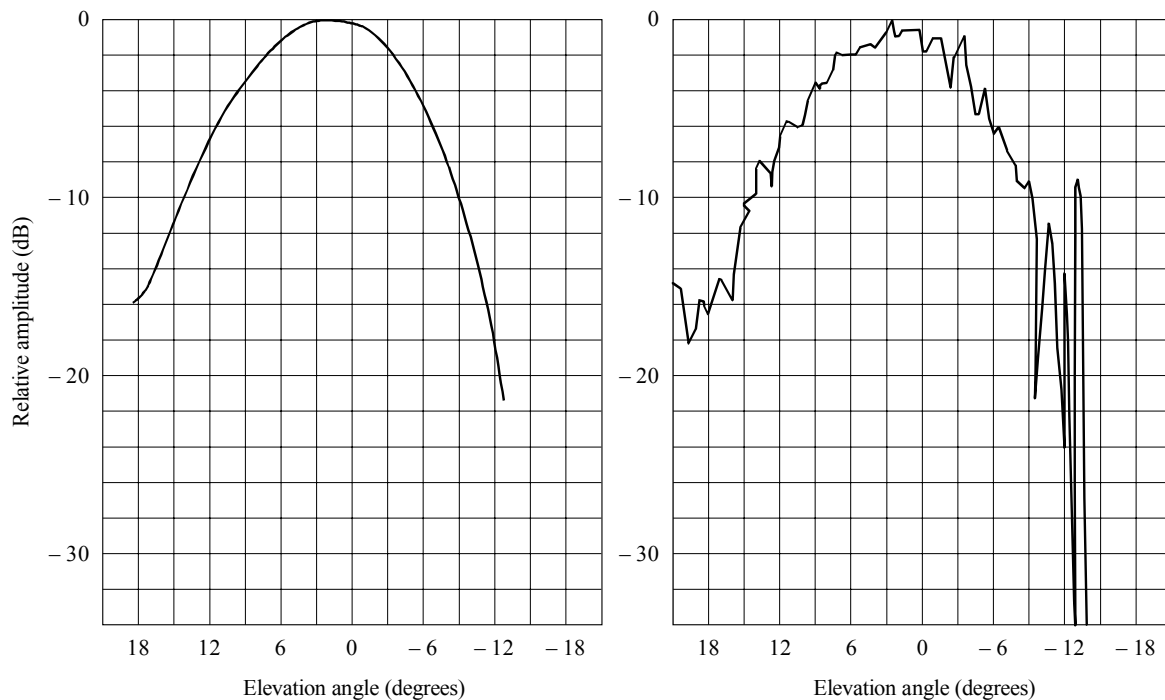
The difference between calculated and measured performance is generally smaller for the individual antenna system element due to easy adjustment of parameters both in VHF and UHF.

In the presence of a complex system, the difference is mainly due to the combined effect of the mechanical and electrical assembly and to the environment in terms of nearby structures. In addition, the presence of buildings can introduce significant differences especially in the vicinity of minimum values, as shown in Fig. 45.

This figure shows the calculated and the measured pattern of a panel antenna system operating at VHF. The discrepancy becomes evident for instance at a depression angle of about  $10^\circ$ , where a value of 10 dB was calculated and a value of about 20 dB actually measured. Reflections from ground and roofs significantly contribute to the shape of the diagram.

FIGURE 45

Calculated and measured vertical patterns



a) Calculated pattern

b) Measured pattern

PART 3  
TO ANNEX 1

## VHF and UHF broadcasting antenna calculation software

### 1 Introduction

This Part describes a practical implementation of a computer program to be used to calculate the antenna system radiation pattern according to the formulae shown in § 7.2 of Part 1.

Appendix 1 to this Part 3 includes the listing of the basic routines to be used in a software package that can be tailored to the specific user's requirements, i.e. for frequency planning, antenna system design, etc.

The hardware requirements will be largely dependent on the software application and may differently affect the minimum hardware implementation that could vary from simple programmable pocket-size calculators to spectrum management mainframe applications.

### 2 Program architecture

The application of the formulae listed in § 7.2 of Part 1 to calculate the radiation pattern of an antenna system requires the availability of a number of input parameters to suitably define the calculation conditions. These parameters may be of a general nature like:

- vision carrier frequency (TV) or channel frequency (FM);
- mid-band operating frequency of the antenna system;
- number and types of the individual antennas composing the antenna system;
- tower cross-section and side length;

and also specific to each individual antenna such as:

- percentage of the applied transmitter power,
- feeding voltage phase,
- tilt angle,
- offset along the tower side,
- vertical spacing between the elements.

Once the type of the individual antennas selected to compose the antenna system is known, their amplitude and phase radiation patterns can be retrieved.

These patterns will have to be previously stored by a specific input program of the package having the task to set up a suitable file containing a digitized representation of the amplitude and phase radiation patterns of the selected individual antennas. This simple program should allow to enter the values of the amplitude and phase of the horizontal and vertical radiation patterns (at maximum gain see § 6.3) given by the manufacturer, with the desired angular resolution. A suitable interpolation will subsequently be used to derive pattern values in directions not coinciding with those used in the sampling process.

By suitable transformation, all the above parameters can define the input necessary to the basic pattern calculation routine listed in Appendix 1. The output of this routine is the e.r.p. value in the desired angular direction specified in terms of azimuth and elevation angles.

APPENDIX 1  
TO PART 3

## Antenna pattern basic calculation subroutine

### 1 Introduction

One of the available functions in the procedure allows to calculate the radiation pattern of an antenna system composed of elementary radiating sources arbitrarily located in a three-dimensional space.

In the present section both the theoretical aspects and the ways to implement the above-mentioned function will be analysed.

The input needed consists in:

- the horizontal and vertical pattern of each elementary source used in the antenna system,
- the geometrical description of the antenna system, i.e. the position and boresight direction of each elementary source,
- description of the power feeding of each source.

The output that can be obtained consists in:

- horizontal radiation patterns at any elevation,
- vertical radiation patterns at any azimuth,
- antenna system gain.

In addition, by means of a graphical representation, it is possible to superimpose some sections of a three-dimensional radiation pattern in order to permit an immediate comparison of the pattern in various directions in space.

The theoretical basis for the calculation of radiation patterns is described below, as well as the translation into a high-level programming language.

### 2 Theoretical basis

Let us assume we have  $N$  radiating sources in a system of Cartesian coordinates x-y-z (see Fig. 46) where:

- the plane x-y is the horizontal plane,
- the axis y is the direction of North in the horizontal plane,
- the axis z is the local vertical.

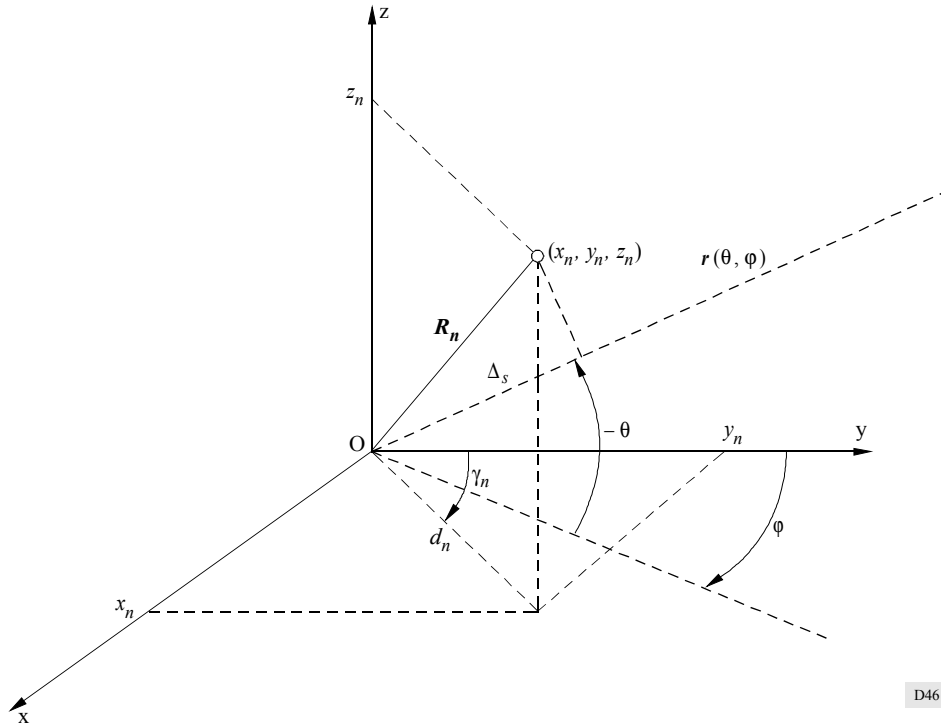
The position of the  $n$ -th radiating source is given by its Cartesian coordinates  $(x_n, y_n, z_n)$  or analogously by the position vector:

$$\mathbf{R}_n = x_n \mathbf{x}_0 + y_n \mathbf{y}_0 + z_n \mathbf{z}_0 \quad (32)$$

The position of the  $n$ -th source can also be expressed in cylindrical co-ordinates  $(d_n, \gamma_n, h_n)$  connected to the corresponding Cartesian coordinates  $(x_n, y_n, z_n)$  through the following relations (see Fig. 46):

$$\begin{aligned} x_n &= d_n \sin \gamma_n \\ y_n &= d_n \cos \gamma_n \\ z_n &= h_n \end{aligned} \quad (33)$$

FIGURE 46



D46

The voltage gain resulting from the composition of the electromagnetic fields of  $N$  radiating sources in the observation direction  $(\theta, \varphi)$  is:

$$G_{Vtot}(\theta, \varphi) = \left| \sum_n \sqrt{a_n} G_{Vn}(\theta, \varphi) e^{j\Delta\Psi_n(\theta, \varphi)} \right| \quad (34)$$

where  $a_n$  is the power percentage feeding of the  $n$ -th radiator, and  $G_{Vn}(\theta, \varphi)$  is its voltage gain in the direction  $(\theta, \varphi)$ , that can be obtained from the horizontal and vertical amplitude pattern of the  $n$ -th source, considering its boresight direction and the rotation around it.

As concerns the phase of the vector in the summation (34), the total phase difference in radians of the  $n$ -th source in the observation direction can be expressed as follows:

$$\Delta\Psi_n(\theta, \varphi) = \Delta\Psi_{n\ pos}(\theta, \varphi) + \Delta\Psi_{n\ diag}(\theta, \varphi) + \Delta\Psi_{n\ el} \quad (35)$$

in which  $\Delta\Psi_{n\ pos}(\theta, \varphi)$  represents the position phase difference (rad) of the  $n$ -th source in the observation direction with respect to a source placed in the origin of the system of coordinates (see Fig. 46) and can be expressed as follows:

$$\Delta\Psi_{n\ pos}(\theta, \varphi) = \frac{2\pi}{\lambda} \Delta s \quad (36)$$

where:

$$\Delta s = (\mathbf{R}_n \cdot \mathbf{r})$$

$\mathbf{R}_n$  is given by (32) and  $\mathbf{r}$  can be expressed, considering that in Fig. 46 the coordinate  $\theta$  is positive in the semispace  $Z < 0$ , as it follows:

$$\mathbf{r} = \cos \theta \sin \varphi \mathbf{x}_0 + \cos \theta \cos \varphi \mathbf{y}_0 - \sin \theta \mathbf{z}_0 \quad (37)$$

By developing the scalar product we obtain the position phase difference of the  $n$ -th source:

$$\Delta\Psi_{n\ pos}(\theta, \varphi) = \frac{2\pi}{\lambda} \left( \cos \theta \sin \varphi x_n + \cos \theta \cos \varphi y_n - \sin \theta z_n \right) \quad (38)$$

Indicating the position of the  $n$ -th source in cylindrical coordinates  $(d_n, \gamma_n, h_n)$  (see expression (33)) the expression (38) becomes:

$$\Delta\Psi_{n\ pos}(\theta, \varphi) = \frac{2\pi}{\lambda} \left( \cos\theta \sin\varphi d_n \sin\gamma_n + \cos\theta \cos\varphi d_n \cos\gamma_n - \sin\theta h_n \right) \quad (39)$$

or analogously:

$$\Delta\Psi_{n\ pos}(\theta, \varphi) = \frac{2\pi}{\lambda} \left[ \cos\theta \cos(\gamma_n - \varphi) d_n - h_n \sin\theta \right] \quad (40)$$

In (35)  $\Delta\Psi_{n\ diag}(\theta, \varphi)$  represents the phase difference (rad) of the phase pattern of the  $n$ -th in the direction  $(\theta, \varphi)$  and  $\Delta\Psi_{n\ el}$  represents the feeding phase difference of the  $n$ -th source that is independent of the observation direction  $(\theta, \varphi)$ .

Developing expression (34) we have:

$$\begin{aligned} G_{Vtot}(\theta, \varphi) &= \left| \sum_n \sqrt{a_n} G_{Vn}(\theta, \varphi) \cos \Delta\Psi_n(\theta, \varphi) + j \sum_n \sqrt{a_n} G_{Vn}(\theta, \varphi) \sin \Delta\Psi_n(\theta, \varphi) \right| = \\ &= \sqrt{\left( \sum_n \sqrt{a_n} G_{Vn}(\theta, \varphi) \cos \Delta\Psi_n(\theta, \varphi) \right)^2 + \left( \sum_n \sqrt{a_n} G_{Vn}(\theta, \varphi) \sin \Delta\Psi_n(\theta, \varphi) \right)^2} \quad (41) \end{aligned}$$

### 3 Calculation software realisation

In order to have a greater flexibility, the procedure was realized with a modular structure and the translation into a high-level programming language is made in C language.

In the following sections the module related to the function  $G_{Vtot}(\theta, \varphi)$  is reported, as well as all the other functions it refers to, utilized for the calculation of the total voltage gain of the antenna system constituted by all the  $N$  radiating sources in the observation direction  $(\theta, \varphi)$ .

#### 3.1 Global variables

Here is the list of the global variables utilized by the modules reported below. A short description of the quantity represented by each variable is also made.

NUMS:	number of radiating sources
TIPO[n]:	type of the $n$ -th radiating source; if all the sources are of the same type TIPO[n]=1 for each $n$
DIAG_AMPH[]:	vector containing the voltage gain, normalized according to the maximum, in the horizontal plane with a 1° step
AMPV_FRONT[]:	vector containing the voltage gain, normalized according to the maximum, in front side of the vertical plane with a 1° step
AMPV_BACK[]:	vector containing the voltage gain, normalized according to the maximum, in the back side of the vertical plane with a 1° step
GVMAX[n]:	maximum voltage gain of the $n$ -th source
LAMBDA_LAV:	wavelength (cm)
FI_O[n], TETA_O[n]:	azimuth and elevation (rad) of the boresight of the $n$ -th radiating source
RIB[n]:	value of the rotation angle (degrees) of the $n$ -th source relative to its boresight direction
POSX[n], POSY[n], POSZ[n]:	Cartesian coordinates of the position of the $n$ -th source (see Fig. 46)
FASE_EL[n]:	phase feed angle of the $n$ -th source (rad)
A[n]:	power feeding coefficient of the $n$ -th source

### 3.2 Calculation functions

#### 3.2.1 DIAG function

This function calculates the voltage gain of “NUMS” radiating sources in the observation direction (FI,TETA). It corresponds to  $G_{V_{tot}}(\varphi, \theta)$ , as described in the theoretical bases.

```

float DIAG(fi,teta)
double fi ,teta;          /* polar co-ordinates (azimuth,elevation) of the observation
                           direction, expressed in radians */
{
  int n;
  double fase_tot;
  double aux0,reale,imag,aux;
  float amp_rad();
  double fase_rad();
  double fase_pos();
  double faseaux;
  reale=0.0;
  imag=0.0;
  for (n=0; n<NUMS;n++)
    {
      fase_tot = fase_rad (fi,teta,n) + fase_pos (fi,teta,n) + fase_el [n];
      aux0 = sqrt(a[n]) * amp_rad (fi,teta,n);
      reale = reale + aux0 * cos(fase_tot);
      imag = imag + aux0 * sin(fase_tot);
    }
  aux = sqrt((reale*reale)+(imag*imag));
  return(aux);
}

```

#### 3.2.2 AMP\_RAD function

This function calculates the voltage gain in the observation direction (FI,TETA) of the  $n$ -th source, considering its horizontal amplitude pattern (DIAG\_AMPH[ ]), its vertical amplitude pattern in the front side (AMPV\_FRONT[ ]) and in the back side (AMPV\_BACK[ ]), and the direction and the rotation of the source. It corresponds to  $G_{V_n}(\varphi, \theta)$ , as described in the theoretical basis.

```

float AMP_RAD(fi,teta,n)
double fi ,teta;          /* polar co-ordinates (azimuth, elevation) of the observation
                           direction, expressed in radians */
int n;                    /* radiating source indicator */
{
  double f2,t2;
  int m;
  int az,abb1,abb2;
  float aux;
  double abb;
  float ampv1,ampv2,ampv;
  m = tipo[n];
  RUOTA_RIB(n,fi,teta,&f2,&t2);
  az = (180./PI)*f2;
  abb = (180./PI)*t2;
  abb1 = abb;
  if (abb1 < 0)
    abb1 += 360;
  abb2 = abb1 + 1;
  if (az1 < 0)
    az1 += 360;
}

```

```

if ((abb1==90)||((abb1==90)))
    az1 = 0;
/* voltage gain of the n-th source in the direction (φ, θ) */
if ((az > 90) && (az < 270))
{
/* interpolation of the value of the amplitude vertical pattern back */
    ampv1 = ampv_back[m][abb1+90];
    ampv2 = ampv_back[m][abb2+90];
    ampv = ampv1 + (ampv2-ampv1)*(abb-abb1);
    aux = gvmax[m]*diag_amph[m][az]*ampv;
}
else
{
/* interpolation of the value of the amplitude vertical pattern front */
    ampv1 = ampv_front[m][abb1+90];
    ampv2 = ampv_front[m][abb2+90];
    ampv = ampv1 + (ampv2-ampv1)*(abb-abb1);
    aux = gvmax[m]*diag_amph[m][az]*ampv;
}
return(aux);
}

```

### 3.2.3 FASE\_RAD function

This function calculates the phase (rad) of the field in the observation direction (FI,TETA) of the  $n$ -th radiating source, considering its phase horizontal pattern (DIAG\_FASEH[ ]), its phase vertical pattern front (FASEV\_FRONT[ ]) and back (FASEV\_BACK[ ]), the direction and rotation of the source.

#### double FASE\_RAD(fi,teta,n)

```

double fi ,teta;          /* polar co-ordinates (azimuth, elevation) of the observation
                           direction, expressed in radians */
int n;                   /* radiating source indicator */
{
    double f2,t2;
    int m,az,abb1,abb2;
    double aux,aux1,aux2,aux3,aux4;
    double abb;
    double fasev1,fasev2,fasev;
    m = tipo[n];

/* calculation of the direction (F2, T2) where to read the n-th source pattern in order to
consider its boresight fi_o[n], teta_o[n] and its rotation around this direction of
rib[n] degree */
    RUOTA_RIB(n,fi,teta,&f2,&t2);
    az = (180./PI)*f2;
    abb = (180./PI)*t2;
    abb1 = abb;
    if (abb1 < 0)
        abb1 += 360;
    abb2 = abb1 + 1;
    if (az1 < 0)
        az1 += 360;
    if ((abb1==90)||((abb1==90)))
        az1 = 0;
    aux1 = diag_faseh[m][0];
    aux2 = diag_faseh[m][180];
    aux3 = fasev_front[m][90];
    aux4 = fasev_back[m][90];
}

```

```

/* phase pattern of the n-th source in the direction ( $\varphi$ ,  $\theta$ ) */
if ((az1 > 90) && (az1 < 270))
{
/* interpolation of the value of the phase vertical pattern back */
fasev1 = fasev_back[m][abb1+90];
fasev2 = fasev_back[m][abb2+90];
fasev = fasev1 + (fasev2-fasev1)*(abb-abb1);
aux = (diag_faseh[m][az]-aux2) * cos(t2) + (fasev - aux4) + aux2 - aux1 ;
}
else
{
/* interpolation of the value of the phase vertical pattern front */
fasev1 = fasev_front[m][abb1+90];
fasev2 = fasev_front[m][abb2+90];
fasev = fasev1 + (fasev2-fasev1)*(abb-abb1);
aux = (diag_faseh[m][az]-aux2) * cos(t2) + (fasev - aux4) + aux2 - aux1 ;
}
aux *= (PI/180.);
return(aux);
}
RUOTA_RIB (n,fi,teta,fout,tout)
double fi ,teta;          /* polar co-ordinates (azimuth, elevation) of the observation
                           direction, expressed in radians */
int n;                   /* radiating source indicator */
double *fout,*tout;      /* polar co-ordinates (azimuth, elevation) of the direction
                           where to read the n-th source pattern in order to consider its
                           boresight and its rotation */

{
float aux;
double trib,fin,tin,arg;
double faux,taux,tgnum,tgden;
int az1,abb1;
/* boresight direction (fi_o[n],teta_o[n]) of the n-th radiating source */
tgnum= cos(teta)*sin(fi-fi_o[n]);
tgden= ( cos(teta)*cos(teta_o[n])*cos(fi-fi_o[n]) + sin(teta)*sin(teta_o[n]) );
fin = atan2(tgnum,tgden);
tin = asin(-cos(teta)*sin(teta_o[n])*cos(fi-fi_o[n]) + sin(teta)*cos(teta_o[n]) );
/* rib[n] degrees continuous rotation of the n-th source */
if (rib[n] != 0)
{
trib = (double) (PI/180.)*rib[n];
faux = atan2( cos(trib)*cos(tin)*sin(fin) - sin(trib)*sin(tin) , cos(tin)*cos(fin) );
arg = sin(trib)*cos(tin)*sin(fin) + cos(trib)*sin(tin);
if (arg >= 1)
    arg = 1.0;
if (arg <= -1)
    arg = -1.0;
taux = asin(arg );
}
else
{
faux = fin;
taux = tin;
}
if (faux>0)
faux += 0.01;
else
faux -= 0.01;
}

```

```

if (taux>0)
    taux += 0.01;
else
    taux -= 0.01;
(*fout) = faux;
(*tout) = taux;
}

```

### 3.2.4 FASE\_POS function

This function calculates the phase difference in the observation direction ( $\varphi$ ,  $\theta$ ) of the  $n$ -th radiating source placed in  $(x_n, y_n, z_n)$  (see Fig. 46).

```

double FASE_POS (fi,teta,n)
double fi ,teta;          /* polar co-ordinates (azimuth, elevation) of the observation
                           direction, expressed in radians */
int n;                   /* radiating source indicator */
{
    double aux;
    double deltas;
    deltas = cos(teta)*sin(fi)*posx[n] + cos(teta)*cos(fi)*posy[n] - sin(teta)*posz[n] ;
    aux = (2*PI/lambda_lav) * deltas;
    return(aux);
}

```

---